JOINT TRANSPORTATION RESEARCH PROGRAM

FHWA/IN/JTRP-2010/26

Final Report

SITE VERIFICATION OF WEIGH-IN-MOTION TRAFFIC AND TIRTL CLASSIFICATION DATA

Shou Li
Yingzi Du
Yi Jiang

December 2010

INDOT Research

TECHNICAL *Summary*

Technology Transfer and Project Implementation Information

TRB Subject Code: 21-7 Safety Appurtenances Design and Placement *December 2010*
Publication No. FHWA/IN/JTRP-2010/26, SPR-3064 *Final Report*

SITE VERIFICATION OF WEIGH-IN-MOTION TRAFFIC AND TIRTL CLASSIFICATION DATA

Introduction

Quality weigh-in-motion (WIM) traffic data is essential not only in general transportation application, but also in pavement design. The new AASHTO Mechanistic-Empirical Pavement Design Guide for New and Rehabilitated Pavement Structures (MEPDG) requires information on the detailed truck traffic, such as truck traffic volume, truck traffic monthly and hourly variations, vehicle class distribution, axle load, and axle load distributions, instead of the traditional ESALs. In addition, the Indiana Department of Transportation (INDOT) needs to collect traffic data frequently so as to timely provide accurate traffic information for planning, program development, operations, and pavement management. Currently, INDOT is using the pneumatic road traffic counters in traffic data collection, such as particular short-term or temporary traffic data collections. However, the pneumatic road traffic counter requires installation of rubber tubes on the pavement surface. As a result, the installation of rubber tubes usually creates safety issues to our workers and is timely consuming and labor intensive. Therefore, it is an urgent need for INDOT to utilize new devices to enhance the safety of field traffic data collection without compromising data quality.

This study consists of two parts. The first part is to verify the accuracy of WIM vehicle classification and develop models for vehicle classification corrections using image processing technologies. The second part is to install and then evaluate a traffic surveillance system, i.e., the Transportable Infra-Red Traffic Logger (TIRTL). In the first part, the investigators collected video and WIM traffic data at WIM sites statewide. A digital image based vehicle monitoring and classification system was developed for verifying weigh-in-station data, in particular the vehicle classification counts. Based on the real world WIM and video traffic classification data, allocation factors were determined for correcting the unclassified vehicle counts associated with the WIM traffic data.

In the second part of this study, a TIRTL system was installed to collect traffic data near a WIM site. Hourly traffic data was first gathered manually and by video cameras to verify the potential errors associated with the TIRTL vehicle counts. Large amount of daily WIM traffic data was also utilized as baseline data to evaluate the field performance of TIRTL and assess the impact of various weather conditions, such as fog, rain and snow, and thunderstorm on TIRTL's performance. The evaluation was based on the FHWA Scheme F Vehicle Classification and solely a data-driven process..

Findings

The digital image based vehicle monitoring and classification system developed by this study is user friendly and can be easily to setup, and perform data acquisition, vehicle monitoring, and length-based vehicle classification. This system can help develop the models for correcting weigh-in-station data, in particular the unclassified vehicle counts. It was shown that the traditional method to treat all unclassified vehicle counts as trucks is too conservative and will largely overestimate the truck traffic volume. Video technologies can provide accurate and effective vehicle detection when vehicles are classified into four categories, including two-axle, four-tire vehicles, single unit trucks, single-trailer trucks, and multi-trailer trucks.

WIM sensor malfunction can generate serious vehicle classification issues. The percentage of unclassified vehicles increases as vehicle counts increases. As the number of travel lanes increases, the possibility for vehicles to execute lane changing or passing increases. Therefore, more vehicles may occupy two adjacent lanes or change speeds on sensors, leading to greater percentages of unclassified vehicles. It becomes unacceptable when the percentage of unclassified vehicles exceeds 4% for a single lane.

Based on the WIM data statewide, the unclassified vehicles mainly involved single tractor trailers and passenger cars. Single unit trucks were most likely classified by WIM. While traffic volume and lane number are the two main contributing factors, it is unrealistic to predict the unclassified vehicles in terms of traffic volume and lane number at this time. Overall, vehicles under Categories 1, 2, 3, and 4 account respectively for 35%, 5%, 48%, and 12% of the total unclassified vehicles.

Under clear weather conditions, the TIRTL vehicle counts agreed very well with the manual and video vehicle counts, respectively. When vehicles are classified into four categories, such as two-axle, four-tire vehicles, single unit trucks, single-trailer trucks, and multi-trailer trucks, the accuracy of vehicle classification for Category 1, including all two-axle, four-tire vehicles, was better than that for tractor trailers. WIM vehicle counts were utilized to validate the performance of TIRTL system. Unlike WIM system, the number of unclassified vehicles by TIRTL was very small.

For axle-based vehicle classification, i.e., the 13-class FHWA vehicle classification scheme, great discrepancies existed between the WIM and TIRTL vehicle class counts. Both WIM and TIRTL demonstrated difficulties to distinguish Class 3 from Class 2. However, TIRTL demonstrated better performance to identify vehicles under Class 3 than WIM, regardless of weather conditions. Under Class 5, the TIRTL vehicle counts were more reasonable than the WIM vehicle counts. The WIM system might over-count vehicles under Class 5. Based on the default truck class distributions, TIRTL might provide vehicle classification more accurate than WIM. Under normal weathers, fog, snow, and rain did not affect TIRTL's performance. Under thunderstorm weather, however, TIRTL might undercount vehicles regardless of vehicle class.

Implementation

The findings on WIM vehicle classification will be utilized by the INDOT Office of Research and Development to adjust truck traffic volumes and vehicle class distribution for the implementation of the new AASHTO MEPDG statewide. The adjustment factors can be used to make corrections on the truck traffic volume and allocate the unclassified vehicles based on vehicle categories.

The findings on TIRTL traffic data collection are intended to assist INDOT Traffic Monitoring Section in assessing the accuracy of TIRTL vehicle classification data and its field performance under various weather conditions. Necessary training will be provided to INDOT pavement designers.

Contacts

For more information:

Shuo Li
Indiana Department of Transportation
Office of Research and Development
West Lafayette, IN 47906
Phone: 765-463-1521
Fax: 765-497-1665
Email: karenzhu@indot.in.gov

Purdue University
Joint Transportation Research Program
School of Civil Engineering
West Lafayette, IN 47907-1284
Phone: (765) 494-9310
Fax: (765) 496-7996
E-mail: jtrp@ecn.purdue.edu
http://www.purdue.edu/jtrp

Joint Transportation Research Program

FHWA/IN/JTRP-2010/26

Site Verification of Weigh-In-Motion Traffic and TIRTL Classification Data

By

Shuo Li, Ph.D., P.E.
Research and Pavement Friction Engineer
Office of Research and Development
Indiana Department of Transportation

Yingzi (Eliza) Du, Ph.D., Assistant Professor
Department of Electrical and Computer Engineering
IUPUI
Indianapolis, IN 46202

And

Yi Jiang, Ph.D., P.E., Associate Professor
Department of Building Construction Management
Purdue University
West Lafayette, IN 47907

Joint Transportation Research Program
Project No. C-36-59XXX
File No. 08-05-50
SPR-3064

Prepared in Cooperation with the
Indiana Department of Transportation and the
U.S. Department of Transportation
Federal Highway Administration

Purdue University
West Lafayette, Indiana 47907
December, 2010

TECHNICAL REPORT STANDARD TITLE PAGE

1. Report No. FHWA/IN/JTRP-2010/26	2. Government Accession No.	3. Recipient's Catalog No.
4. Title and Subtitle Site Verification of Weigh-In-Motion Traffic and TIRTL Classification Data		5. Report Date December 2010
		6. Performing Organization Code
7. Author(s) Shuo Li, Yingzi (Eliza) Du, Yi Jiang		8. Performing Organization Report No. FHWA/IN/JTRP-2009/26
9. Performing Organization Name and Address Joint Transportation Research Program 1284 Civil Engineering Building Purdue University West Lafayette, Indiana 47907-1284		10. Work Unit No.
		11. Contract or Grant No. SPR-3064
12. Sponsoring Agency Name and Address Indiana Department of Transportation State Office Building 100 North Senate Avenue Indianapolis, IN 46204		13. Type of Report and Period Covered Final Report
		14. Sponsoring Agency Code

15. Supplementary Notes
Prepared in cooperation with the Indiana Department of Transportation and Federal Highway Administration.

16. Abstract

Quality weigh-in-motion (WIM) traffic data is essential not only in general transportation application, but also in pavement design. The new AASHTO Mechanistic-Empirical Pavement Design Guide (MEPDG) for New and Rehabilitated Pavement Structures requires information on the detailed truck traffic, such as truck traffic volume, truck traffic monthly and hourly variations, vehicle class distribution, axle load, and axle load distributions, instead of the traditional ESALs. In addition, the Indiana Department of Transportation (INDOT) needs to collect traffic data frequently so as to timely provide accurate traffic information for planning, program development, operations, and pavement management. Currently, INDOT is using the pneumatic road traffic counters in traffic data collection, such as particular short-term or temporary traffic data collections. However, the pneumatic road traffic counter requires installation of rubber tubes on the pavement surface. As a result, the installation of rubber tubes usually creates safety issues to our workers and is timely consuming and labor intensive. Therefore, it is an urgent need for INDOT to utilize new devices to enhance the safety of field traffic data collection without compromising data quality.

This study consists of two parts. The first part is to verify the accuracy of WIM vehicle classification and develop models for vehicle classification corrections using image processing technologies. The second part is to install and then evaluate a traffic surveillance system, i.e., the Transportable Infra-Red Traffic Logger (TIRTL). In the first part, the investigators collected video and WIM traffic data at WIM sites statewide. A digital image based vehicle monitoring and classification system was developed for verifying weigh-in-station data, in particular the vehicle classification counts. Based on the real world WIM and video traffic classification data, allocation factors were determined for correcting the unclassified vehicle counts associated with the WIM traffic data.

In the second part of this study, a TIRTL system was installed to collect traffic data near a WIM site. Hourly traffic data was first gathered manually and by video cameras to verify the potential errors associated with the TIRTL vehicle counts. Large amount of daily WIM traffic data was also utilized as baseline data to evaluate the field performance of TIRTL and assess the impact of various weather conditions, such as fog, rain and snow, and thunderstorm on TIRTL's performance. The evaluation was based on the FHWA Scheme F Vehicle Classification and solely a data-driven process.

17. Key Words	18. Distribution Statement
Weigh-in-motion, vehicle tracking, traffic monitoring, dynamic content based image segmentation, vehicle classification, infra-red light technology, weather condition	No restrictions. This document is available to the public through the National Technical Information Service, Springfield, VA 22161

19. Security Classif. (of this report)	20. Security Classif. (of this page)	21. No. of Pages	22. Price
Unclassified	Unclassified	60	

Form DOT F 1700.7 (8-69)

TABLE OF CONTENTS

LIST OF TABLES

LIST OF FIGURES

ACKNOWLEDGMENTS

This research project was sponsored by the Indiana Department of Transportation (INDOT) in cooperation with the Federal Highway Administration through the Joint Transportation Research Program (JTRP). The authors would like to thank the study advisory committee members, Kirk Mangold, Tommy Nantung, and Samy Noureldin for their valuable assistance and technical guidance in the course of performing this study. Sincere thanks are extended to Larry Torrance of the INDOT and Robb Bingham of Control Specialists Company for their assistance in data collection and system evaluation.

Chapter 1

INTRODUCTION

Background

In the past decades, vehicle classification data has been widely used in transportation planning, highway operations, traffic analysis, and performance measurements. This data serves as the starting point for other needed transportation statistics, including truck vehicle miles traveled (VMT), and freight tonnage carried by trucks along certain roadways or on the whole highway network. In addition, this data has been utilized to estimate the traffic load design inputs such as equivalent single axle loads (ESALs) for pavement structural design and to calculate the pavement remaining life for pavement management systems. Recently, a new pavement design guide, the AASHTO Mechanistic-Empirical Pavement Design Guide (MEPDG) (1) was released as a tool for the design and analysis of new and rehabilitated pavement structures.

The AASHTO MEPDG utilizes a comprehensive suite of design inputs to design pavements with enhanced reliability and desired performance. The traffic input approach in the MEPDG is more consistent with the state-of-practice for traffic monitoring outlined in the FHWA Traffic Monitoring Guide (TMG) (2). It becomes possible for state highway agencies (SHAs) to develop a harmonious and integrated traffic database that can be used not only for transportation applications such as planning and programming, but also for pavement structural design and analysis. However, SHAs are facing great challenges to implement the MEPDG due to the considerable amount of design inputs needed and the selection of the corresponding reliability level for each pavement project. As an illustration, the MEPDG requires information on the detailed truck traffic volume, truck traffic monthly and hourly variations, vehicle class distribution, and axle load distributions, instead of the sole traffic input, i.e., ESALs.

In an effort to address the implementation issues and to make those advantages become real, the INDOT Office of Research and Development has initiated research activities for possible implementation of the AASHTO MEPDG. As part of the effort, initiatives have been undertaken to assess potential issues that may arise from traffic data acquiring and processing, and to assess technologies and data needs to meet the traffic input requirements of the MEPDG (3). Considerable work has been done to process the weigh-in-motion (WIM) data collected at all WIM sites statewide. Traffic data input architecture has been established. Updated knowledge has been achieved on the characteristics of truck traffic and truckloads. Preliminary results have been recommended to the INDOT Pavement Design Committee and findings have been presented at TRB annual meetings to share our knowledge and experience with other SHAs.

Problem Statement

Data quality plays an important role in identifying truck traffic design inputs that are required in the MEPDG. Joint efforts have been made by INDOT and Purdue University to ensure WIM data quality (4). However, the algorithms used for WIM vehicle classification may not function properly in some occasions. As a result, many vehicles may not be classified. Figure 1 shows the counts of vehicles that were not classified. At the two WIM sites on US-41 and I-65, the unclassified vehicle counts are almost constant over time. On the Borman Expressway site, however, the unclassified vehicle count varied from time to time and accounted for more than 30% of the total vehicle count in October. It is possible that the setting of the time-out or vehicle-length threshold might be inappropriate. However, other factors such as involvement of multiple vehicles will also create an axle configuration that is not defined in the WIM system. In addition, it appears that both traffic volume and number of lanes have an impact on vehicle classification.

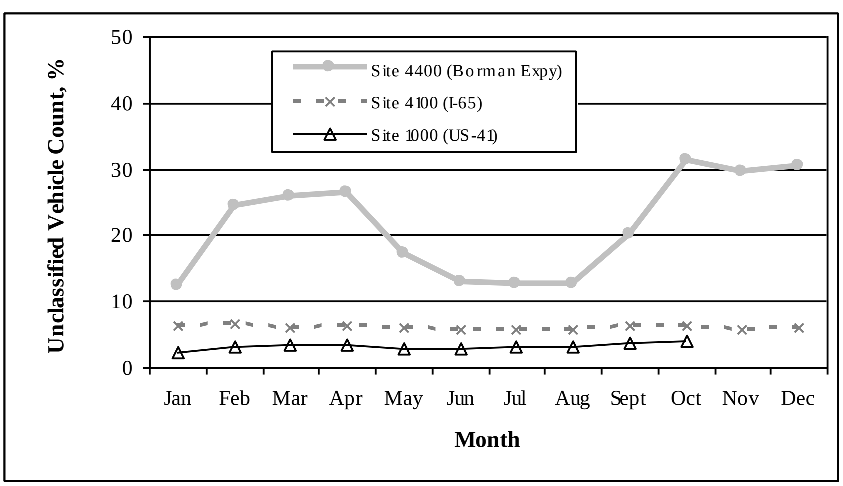

Figure 1 Unclassified Vehicle Counts

As a general practice, SHAs usually assign those unclassified vehicles to pre-determined truck classes. Consequently, the truck traffic is usually overestimated and the resulting pavement structures may become very conservative. In order to evaluate the effect of unclassified vehicles on the pavement design, the MEPDG analysis software was utilized to examine the pavement performance on different highways by assuming a percentage of 5%, 10%, 20%, and 30% for the unclassified vehicles. As presented in Figure 2 are the predicted pavement distresses, such as longitudinal cracking and alligator cracking. Both longitudinal cracking and alligator cracking increase as the unclassified vehicle count increases. Apparently, it is a significant need to verify the WIM vehicle classification using alternative and more accurate approaches.

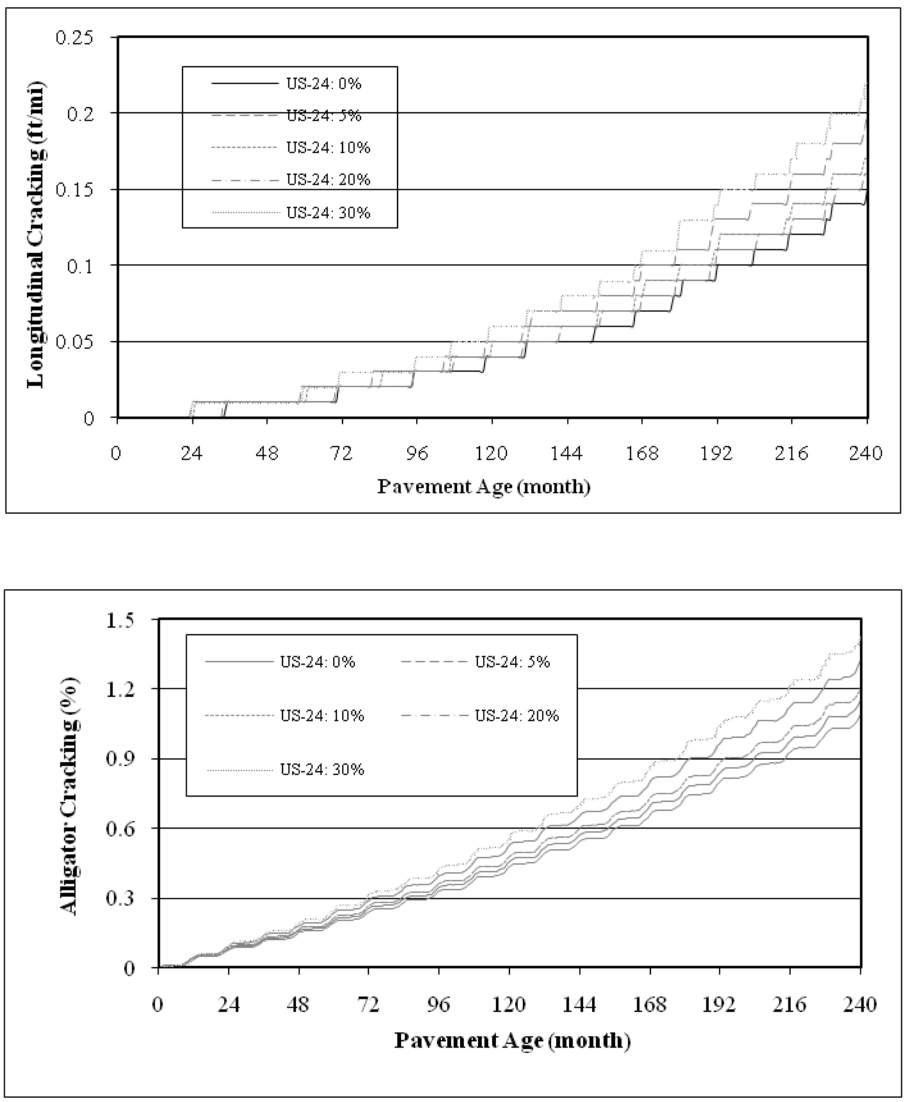

Figure 2 Effects of Unclassified Vehicles on Pavement Cracking

In addition, INDOT Planning needs to collect traffic data frequently so as to timely provide accurate traffic information for planning, program development, operations, and pavement engineering. Currently, INDOT is using the pneumatic road traffic counters in traffic data collection, such as particular short-term or temporary traffic data collections. However, the pneumatic road traffic counter requires installation of rubber tubes on the pavement surface. As a result, the installation of rubber tubes usually creates safety issues to our workers, in particular on the high-speed highway facilities. Also, the installation of rubber tubes is time consuming and labor intensive. It takes approximately six man-hours to install the tubes on a four-lane interstate highway. Recently, INDOT started to experiment a traffic data collection device, i.e., Transportable Infra-Red Traffic Logger (TIRTL) (5). While it was reported that TIRTL can support a variety of applications for data collection and its installation is non-invasive, no firsthand information is available on the concerns about field installation, data accuracy and reliability, in particular the field performance under unfavorable conditions.

Objectives

The objectives of this study are threefold: (a) to implement emerging technologies developed to verify the accuracy of WIM vehicle classification; (b) to develop implementation models based on the main factors such as the number of lanes, traffic volume, and truck percentage to generate correction factors for unclassified vehicles; and (c) to evaluate the field performance of TIRTL under different conditions. It is expected that once the objectives are fulfilled, this study can provide more reliable WIM data for pavement design and other transportation applications, and enhance the safety of field traffic data collection without compromising data quality.

Main Tasks and Research Approach

Synthesis Study

This study will conduct a literature review to examine the algorithms for WIM vehicle classification, the effect of WIM setting on the accuracy of vehicle classification, and the potential issues on the use of image technologies for traffic data collection and vehicle classification. This study will also review the signal producing and processing technologies related to the proposed traffic counter/classifier, TIRTL. The synthesis will focus on resources such as FHWA reports, state highway agency reports, TRB papers, ASTM standards, NCHRP studies, and FHWA Long-Term Pavement Performance (LTPP) Specific Pavement Study (SPS) Traffic Pooled Fund Study TPF-5(004).

WIM, Image, and TIRTL Traffic Data Collections

In order to verify the accuracy of WIM vehicle classifications and evaluate the performance of the proposed device, WIM, image and TIRTL traffic data will be collected on selected WIM or automatic vehicle classification (AVC) sites. The selection of WIM sites will take into account many factors, such as highway class, number of lanes, traffic volume and truck percentage. The pre-determined WIM sites will be those on highways with one to three lanes in one direction, such as Borman Expressway, I-65, I-465, I-74, US-24, and US-31, so as to produce representative solutions for highways in Indiana. The WIM traffic data will be collected using the existing WIM systems. The image traffic data will be collected at the selected WIM sites using video cameras during different hours such as peak hours and non-peak hours. The vehicle count/classification data using TIRTL will take into account the effects of time period, traffic volume and weather conditions.

Automatic Traffic Data Classification Using Image Processing Technologies

In the project, an automatic traffic data classification system using image processing technologies will be developed / implemented. This proposed system will consist of six stages:

- Video Image Acquisition: acquire video images containing traffic data
- Image De-noising: remove the noise occurred during data collection
- Image segmentation: segment the vehicles out from the video images
- Region Tracking: track interested regions over a sequence of images using spatial corrections between video frames.
- Object Classification: This step will classify the vehicles into three different classes: passenger vehicles, single-unit trucks, and combination trucks.
- Output: Output the classification results.

This Image-based traffic data classification system can offer a number of advantages over current approaches: First, lane changes can be detected and counted in the classification. Second, the tracking function provides dynamic information of moving vehicles, which can improve the accuracy of vehicle classification. Third, the accuracy of this system can be verified by human operators using a manual counting/classification method. Finally, this system is easy to deploy.

Data Analysis

The WIM and image traffic data collected simultaneously will be examined to verify the accuracy of WIM vehicle classification and identify the unclassified vehicles. The developed automatic traffic classification system based on image processing technologies will be utilized to accomplish this task. Sensitivity analysis will be conducted to evaluate the effect of traffic characteristics and highway lane geometrics on the accuracy of WIM vehicle classification and to determine the potential patterns or trends associated with the variation of the unclassified vehicle count. The traffic data collected using TIRTL and AVC system (or image equipment or WIM) will be examined in light of the time period, number of lanes and weather.

Model Development and Verification

Models will be developed to generate correction factors for unclassified vehicle counts with respect to potential factors such as the number of lanes, traffic volume, truck percentage and to assign the unclassified vehicles to the pre-determined vehicle classes. The models will be verified using the WIM and image traffic data collected on other highways.

Performance Evaluation of TIRTL

The performance of the proposed device, TIRTL, will be evaluated so as to examine not only the unit system errors, but also the accuracy and reliability under different road, traffic and weather conditions, including roadside and median ground vegetation, peak and off-peak hour, daytime and nighttime, raining and snowing. Comparative data will be collected using different methods, such as manually, using TIRTL, from WIM site, and using video camera. This study will also evaluate the long-term performance of TIRTL for possible use in place of other AVC devices at some permanent sites or for possible use as a support for WIM systems in vehicle classification and counting.

Report

The study approaches, data, and results will be documented. Computer program and models will be available for verifying vehicle classification when the project is completed. Recommendations will be made for correcting WIM vehicle classification data and use of the proposed device in traffic data collection.

Chapter 2

DEVELOPMENT OF DYNAMIC CONTENT BASED VEHICLE TRACKING AND TRAFFIC MONITORING SYSTEM

Overview

Traffic data may be obtained from different vehicle sensing technologies, such as loop detectors, microwave radars, infrared detectors, and laser sensors. With the rapid advance of video camera and computer technologies, the application of vision-based vehicle monitoring system has been increasing dramatically. Compared to the vehicle sensing technologies, in particular loop detectors, the vision-based vehicle monitoring system offers a number of advantages. First, the vision-based vehicle monitoring system is more economic and easy to install. Second, this monitoring system serves as a real-time vehicle observer and provides useful video data for a variety of field traffic studies, in particular for validation of other vehicle sensors. Third, a larger set of traffic parameters such as lane changing, congestion, and accidents, can be obtained and measured based on the information content associated with image sequences. In contrast, the loop detectors are limited to a spot where they are deployed. In addition, the cameras are easier to install as well as less costly.

Video image processing based vehicle tracking and traffic monitoring has been an active research topic in computer vision and image processing. Baker et al. used a feature-based method with occlusion reasoning for tracking vehicles in congested traffic scenes (6, 7). This approach is computationally expensive. Karmann et al. used adaptive background subtraction method to track moving vehicles (8). Subtracting the background is a popular technique for moving object tracking. The differences are in how to obtain the background and how to subtract it. Masound et al. adapted a similar approach with lane change tracking (9). Later on, Gupte et al. adopted a similar concept and developed a vehicle detection and classification scheme based on instantaneous backgrounds (10).

Karmann et al. defines the background to be a slow, time-varying image sequence, while Gupte et al. updates the background by adding the weight of the current background obtained from the current frame to the previous background. The key step in vision-based systems is image segmentation. Traditionally, the segmentation is often assumed to be able to accurately extract the object of interest from the background image autonomously. Existing image segmentation algorithms assume (11): 1) The region of the object of interest is uniform and homogeneous; 2) Adjacent regions should be differing significantly.

But for vehicle tracking, these traditional assumptions are often wrong. Figure 2-14(a) shows an example of a cargo truck with a number of cars attached to the trailer. It should be only counted as one vehicle. However, this region of this object is neither uniform, nor homogeneous. Figure 2-14 shows an example to a group of same kind of trucks. They are two vehicles. But the characteristics of the two objects are very close to each other; these two are connected as one region in the scene. As a result, the connected region is uniform and homogenous. It would be detected as one region if assumption 2 is used.

a) A cargo truck with non-uniform/non-homogeneous characteristics

b) A group of same kind of tucks on the road.

Figure 2-14 The Problems of the Traditional Segmentation Assumptions

Content-based image segmentation methods have different approaches. They segment the image based on the characteristics/features of the targeted object. Fuh et al. uses relationship tree matching approach to achieve hierarchical color region segmentation (12). This approach is designed for content based image information retrieval. Chen et al. proposed adaptive perceptual color-texture based method (13). It aimed at segmentation of nature scenes. Gevers uses matching feature distribution based on color gradients for content-based image retrieval of textured objects under nature scenes (14). Sun et al. proposed semiautomatic video object segmentation using vsnakes (15). This approach needs the semantic object initialization with human assistance. Farmer et al. proposed a wrapper-based approach for image segmentation and classification (16). In this approach, the shape of the desired object is used in feature extraction and classification as an integrated part of image segmentation.

However, none of the above methods will be suitable for our application. Vehicles on the highway may have very different shapes. Figure 15-2 shows the 13 classes by the Federal Highway Administration (FHWA). In real life, individual vehicles in the same class can be very different.

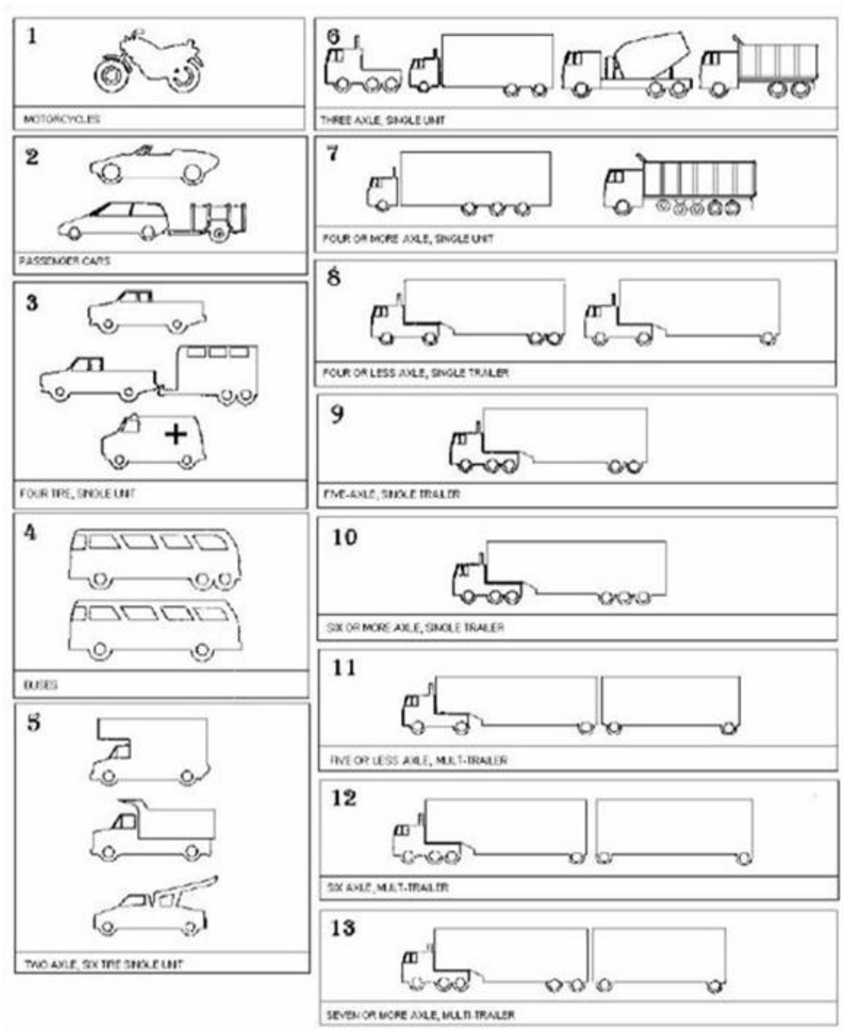

Figure 15-1 FHWA 13 Vehicle Classes

Traditional Vehicle Categories

In the FHWA vehicle classification scheme (2), vehicles are divided into 13 classes in light of vehicle dimension and axle characteristics as shown in Figure 2-2. Because of the complications of real-life vehicle sizes and the difficulties of field video image acquisition, it is unrealistic to identify the class of each individual vehicle and provide the results using all 13 FHWA vehicle classes. On the one hand, vehicle sizes and axle characteristics vary significantly even in the same class. On the other hand, the effects of all passenger vehicles are negligible on pavement structures and only vehicles of Classes 4-13 are considered in pavement design. In particular in the process of estimating the equivalent-single axle loads (ESALS) (17), each individual truck is converted into a certain number of ESALS simply based on the truck is a single unit truck or a tractor trailer.

In this study, one of the main goals is to validate the WIM vehicle classification data and examine the classes of those unclassified vehicles. To be compatible both with the FHWA vehicle classification and the primary interest of pavement design, vehicles are further grouped into four broad, traditional categories as shown in Table 2-1. Category 1 includes all passenger vehicles of Classes 1-3. Category 2 consists of all single unit trucks, such as vehicles of Classes 4-7. Category 3 consists of all single tractor trailers, including vehicles of Classes 8-10. Vehicles of Classes 11-13 are multi-trailer trucks and are grouped into Category 4.

Table 2-2 Four Traditional Vehicle Categories

Vehicle Category	FHWA Vehicle Classes
1	Classes 1, 2, and 3
2	Classes 4,5, 6 and 7
3	Classes 8,9, and 10
4	Classes 11, 12, and 13

Approach for Digital Image Processing

In this study, the dynamic content based image segmentation method was employed for developing the vehicle tracking and traffic monitoring system. The digital image processing approach in this system consists of six stages, such as video image acquisition, lane selection, image preprocessing, dynamic content-based image segmentation and region tracking, vehicle counting, vehicle classification, and output

Image Acquisition

Traditional vehicle classification and tracking systems use industry graded cameras and mount the cameras in a very high and fixed location. The benefits of this kind of image acquisition systems are:

- It is very easy to model the vehicle in the image since the projection is fixed.
- The image tends to have higher quality and less noise.
- The cameras are mounted high, and can have unblocked view of the vehicles.

In this study, it is needed to have an acquisition system that can be easily moved around, easily setup without blocking/affecting the traffic, and can acquire the data at any angle. However, this kind of sitting would not work for this project because it is hart to move and mount. This study developed an image acquisition system that uses camcorder (customer electronics), which is light weight, easy to mount and move. In this system, the SONY DCR-SR100 Handycam hard drive camcorder is used. The acquired videos can be directly saved in the camcorder.

To connect the camcorder with the computer, this study further designed a Matlab Graphic Unser Interface (GUI) to allow users to easily acquire the data from the camera to the computer in real-time. If the users prefer to acquire the data first and process the data off-line, the system also provides such capability. The users can choose "load data" and then process.

Lane Selection and Data Projection

There are two ways for lane selection: automatic lane selection or manual lane selection. In the literature, when designing the automatic lane selection, the authors often assumes that the vehicles will be stay in the same line all the time, or assumes that the parameters of the camera location are known. Both are not practical in this project.

The lane selection is one of the most important initial steps in this system. It is important to have accurate selection and adapt to any kinds of camera settings. Therefore, in this project, the manual selection approach was used. After connecting the camcorder with the computer using Matlab GUI, the "lane selection" button will be visible for the users to select. The users can input the total number of lanes in the video image and use mouse to select the lane boundaries. The process is fast and easy. With user interfering, it is much more accurate.

Image Preprocessing

In this study, in order to ensure the entire system is easy to move and setup, a Laptop was used. The processing power of the laptop is far less than that of the high end computing equipment used in many researchers in this area. The image resolution of each frame is about 1M, and 30 frames per second. This results in a lot of data for processing. In this project, to ensure that the laptop can process the data in real-time, the image was down sampled to improve the speed. This downsampling process can greatly reduce the process speed, but at same time, it makes it much more challenging in the image processing step.

In this study, the system can work on any video images with the resolution of each frame is more than 20K pixels (around 100x200), frame speed more than 15 frame/second.

Dynamic Content-Based Image Segmentation

The dynamic content-based image segmentation is performed as follows:

(a) Background Calculation. The first step to segment the region of interest is to calculate and update the background. This method should be robust enough for accurate vehicle segmentation. At the same time, it should be fast enough to operate. In this study, the background was updated for every N frames. N can be chosen by the users. The smaller the N is, the more often the update would be. However, it will take more computation time. If N is too big, there will be long-delays in the background update. By taking two consecutive video frames, and subtracting them, only the objects in the frames which are moving will produce non-zero pixel values in the resulting difference image. Once the difference image is produced, the R, G, and B layers are turned into binary images where Ix(i,j) is the pixel value at (i,j), Lx is the binary image, and x is either R, G, or B. The frame subtraction method is summarized with the flow chart in Figure 2-16.

(b) Preliminary Segmentation. Preliminary segmentation serves two functions: 1) remove the background from the current video frame; and 2) threshold the image to find potential regions of interest.

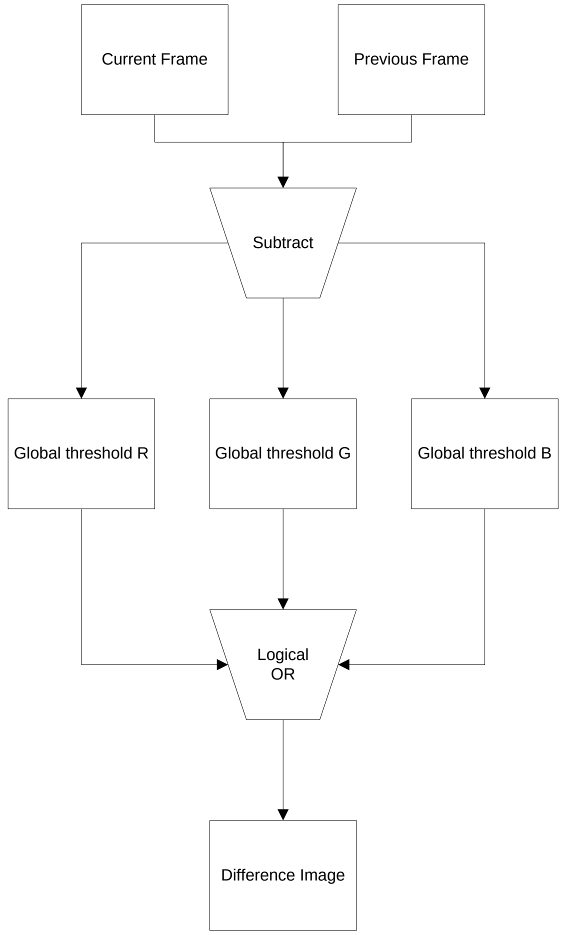

Figure 2-16 Flow Chart for the Frame Subtraction Method

The preliminary segmented image is calculated by:

$$g_i(x,y) = \begin{cases} 1, & \text{if } s_i(x,y) > T \\ 0, & else \end{cases} \tag{2-1}$$

where, T is the threshold, and $s_i(x,y)$ is the subtraction result:

$$\boldsymbol{s_i(x,y) = dc(f_i(x,y), bk(x,y))}\,. \tag{2-2}$$

where, $\boldsymbol{dc(f_i(x,y), bk(x,y))}$ is the color distance, i.e. the Euclidean distance in RGB; $\boldsymbol{f_i(x,y)}$ i the pixel (x,y) in the ith input image; and $\boldsymbol{bk(x,y)}$ is the pixel (x,y) in the background image.

Color distance $dc\left(h_1(x,y), h_2(x,y)\right)$ between pixel $h_1(x,y)$ and $h_2(x,y)$ is calculated by:

$$dc\left(h_1(x,y), h_2(x,y)\right) = \sqrt{\left(h_1^{r}(x,y) - h_2^{r}(x,y)\right)^2 + \left(h_1^{g}(x,y) - h_2^{g}(x,y)\right)^2 + \left(h_1^{b}(x,y) - h_2^{b}(x,y)\right)^2} \quad (2\text{-}3)$$

in which, $h_1^{r}(x,y)$, $h_1^{g}(x,y)$, and $h_1^{b}(x,y)$ are red, green, and blue dimensions of the pixel (x,y) of image h_1 respectively. $h_2^{r}(x,y)$, $h_2^{g}(x,y)$, and $h_2^{b}(x,y)$ are red, green, and blue dimensions of the pixel (x,y) of image h_2, respectively.

(c) Content-Based Region Connection. At this step, the small areas are first eliminated to reduce the noise blocks. The purpose of region connection is to connect the regions that are possibly from same vehicle. The region of a vehicle in an image is often neither uniform, nor homogeneous. In this project, the two regions will be connected based on their location, and similarities of boundary characteristics. Any two regions will be connected if and only if they satisfy the following three rules:

Rule A-The centers of the regions are in a same lane. The center of the regions is calculated by:

$$\begin{aligned} C_x^m &= \min\{x \mid g(x,y) \in R_m\} + \max\{x \mid g(x,y) \in R_m\} \\ C_y^m &= \min\{y \mid g(x,y) \in R_m\} + \max\{y \mid g(x,y) \in R_m\}. \end{aligned} \quad (2\text{-}4)$$

where, (C_x^m, C_y^m) is the coordinate of the center for mth region. In this way, the holes in an imperfectly separated region are ignored.

In this study, it was assumed that the lanes are straight lines. The linear model of each lane boundaries, Eq. (3), is calculated from initial camera calibration parameters:

$$y = kx + b \quad (2\text{-}5)$$

$$(C_x^m, C_y^m) \in L_i, \text{ if } \min_i \left(D\left((C_x^m, C_y^m), LB_{i,1}\right) + D\left((C_x^m, C_y^m), LB_{i,2}\right)\right) \quad (2\text{-}6)$$

where, $D(\!(x,y), LB_{j,k})$ is the shortest distance from the point (x,y) to the jth lane LB_j's kth boundary line $LB_{j,k}$ (Each lane has two boundary lines).

Rule A is to test if both the center of mth region (C_x^m, C_y^m) and the center of nth region (C_x^n, C_y^n) belong to a same lane using Eq. (2-6).

Rule B-The distance of the regions is smaller than the threshold T_d. The distance of the centers from two different regions is calculated using Euclidean distance:

$$d_{mn} = \begin{cases} \sqrt{(C_x^m - C_x^n)^2 + (C_y^m - C_y^n)^2}, & (C_x^m, C_y^m) \in L_i \ \& \ (C_x^n, C_y^n) \in L_j \\ \infty, & \textit{otherwise} \end{cases}. \quad (2\text{-}7)$$

where, L_i and L_j represent the areas of ith and jth lanes.

Rule C-The boundaries of the two regions have similar characteristics in the close up side. Traditionally, the regions with similar characteristics in the entire areas are connected. This is based on the assumption that the object has uniform/homogenous characteristics. In this study, use the characteristics of the close side of boundaries of the regions, instead of the entire areas or entire boundaries, were used. This relaxes the requirement of uniformity or homogeny characteristics of the object or the boundaries of the object.

If the average color of the close up side satisfies $dc(B_i, B_j) < T_{bc}$, the two regions satisfy Rule C. T_{bc} is the threshold. B_i and B_j are the average colors of the close up side for region *i* and *j*. To connect two regions, the gaps are bridged between two close-up boundaries. The region labels will be updated after connecting regions.

(d) Content-based Region Separation. Some regions may cross more than one lane in a video frame, which may be from the same vehicle as shown in Figure 2-17(a) or multiple vehicles as shown in Figure 2-17(b). Proper disconnecting of the regions from multiple vehicles is necessary for accurate traffic count. At the same time, the region from a single vehicle (crossing multiple lanes) should be kept in one piece. The content-based region separation is made with the following four steps:

(a) One vehicle cross two lanes **(b) Two vehicles cross three lanes**

Figure 2-17 Examples of Vehicles over Multiple Lanes

- The region was separated into sub-regions based on the boundaries of the lanes. For each sub-region, if the area is small, this region will be eliminated.
- Calculate the mass centers (which is different from Eq. 4) of the sub-region by:

$$\boldsymbol{M}_x^{j,i} = \sum_{f(x,y)\in S_i^j} \boldsymbol{x} \quad \text{and} \quad \boldsymbol{M}_y^{j,i} = \sum_{f(x,y)\in S_i^j} \boldsymbol{y} \qquad (2\text{-}8)$$

where, ($\boldsymbol{M}_x^{j,i}, \boldsymbol{M}_y^{j,i}$) is the mass center of the *i*th sub-region of Region j, $\boldsymbol{S}_i^j$.

- Calculated the shortest distance from the mass center of this region to the lane boundaries $\boldsymbol{D}((\boldsymbol{M}_x^{j,i}, \boldsymbol{M}_y^{j,i}), \boldsymbol{LB}_{n,1})$ and $\boldsymbol{D}((\boldsymbol{M}_x^{j,i}, \boldsymbol{M}_y^{j,i}), \boldsymbol{LB}_{n,2})$ respectively. Here the sub-region $\boldsymbol{S}_i^j$ is in the nth lane.
- Decide if this sub-region should stay or disappear by:

$$\delta_i^j = \begin{cases} 1, & \left|\boldsymbol{D}((\boldsymbol{M}_x^{j,i}, \boldsymbol{M}_y^{j,i}), \boldsymbol{LB}_{n,1}) - \boldsymbol{D}((\boldsymbol{M}_x^{j,i}, \boldsymbol{M}_y^{j,i}), \boldsymbol{LB}_{n,2})\right| > \mathrm{T_d} \\ 0, & \textbf{\textit{else}} \end{cases} . \qquad (2\text{-}9)$$

where, T_d is the threshold for the distance. If δ_i^j =1, the sub-region $\boldsymbol{S}_i^j$ should be eliminated. Otherwise, the sub-region $\boldsymbol{S}_i^j$ should be separated as a new region.

Figure 2-18(e) and 2-5(f) show the region separation results based on Eq. (2-8). After the region separation, the regions are relabeled.

(a) Original

(b) Downsampled

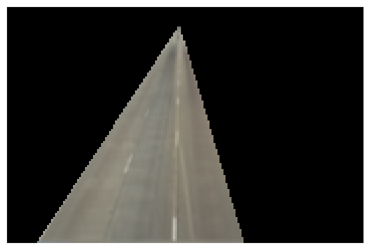

(c) Calculated Background Image

d) Subtraction of Background Image

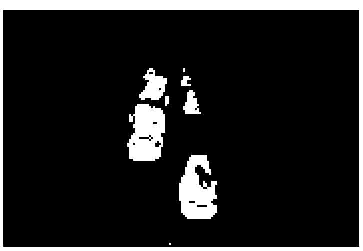

e) Threshold of Subtraction Frame

f) Cleaned Threshold

g) Adjacent Cars Separation

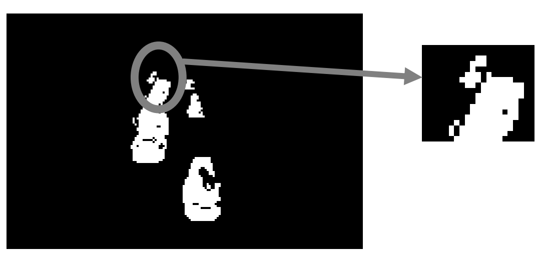

h) Joined Regions (Final Segmentation Results)

Figure 2-18 Illustration of the Separation Process

(e) Reconnect the Regions. After region separation, it is needed to check if there are regions that satisfy the three rules in the section of Content-Based Region Connection, and connect those regions.

(f) Dynamic Region Tracking. In this step, it is to find the moving direction of the regions by finding the related location of in two consecutive video frames. If the entire region areas are used to track the vehicle, there will be more computation complexity. Moreover, lane changing, or other abnormal traffic patterns can be miss-identified. In this study, the center-tracking method was employed.

If two regions from two consecutive video frames have certain a percentage of overlapping, two regions are from same vehicle. Suppose $\boldsymbol{R}_{\boldsymbol{n}}^{\boldsymbol{i}-1}$ and $\boldsymbol{R}_{\boldsymbol{m}}^{\boldsymbol{i}}$ are from same vehicle. $(\boldsymbol{C}_{\boldsymbol{x}}^{\boldsymbol{n}}, \boldsymbol{C}_{\boldsymbol{y}}^{\boldsymbol{n}})^{\boldsymbol{i}-1}$ and $(\boldsymbol{C}_{\boldsymbol{x}}^{\boldsymbol{m}}, \boldsymbol{C}_{\boldsymbol{y}}^{\boldsymbol{m}})^{\boldsymbol{i}}$ are the centers for $\boldsymbol{R}_{\boldsymbol{n}}^{\boldsymbol{i}-1}$ and $\boldsymbol{R}_{\boldsymbol{m}}^{\boldsymbol{i}}$ respectively. The moving direction of the vehicle is decided by the location of the centers. By tracking vehicle movement of initial video frames, the traffic patterns can be determined for each lane.

<u>Dynamic Vehicle Counting</u>

To count the vehicle accurately, it is needed to avoid multiple counts of the same vehicle, or miss-counting of any single vehicle. In real life, the patterns of the traffic may be abnormal, for example, a vehicle may stop in the middle of driving for mechanical problems. Since, in this system, our camera is setup to monitor the incoming or outgoing traffic, an invisible counting line is initialized horizontally close the bottom of the video image. However, this invisible counting line can be initialized vertically if the vehicles are in a side view.

Using the method described in the section of Dynamic Region Tracking, the movement of the center can be monitored for each vehicle. For our cases, the camera is setup to take incoming or outgoing patterns of the traffic. Only when the center of the vehicle passes the counting line in the similar direction of a traffic patterns for that lane, the vehicle will be counted. To validate our approach, a single video camera was set up on a tripod (6 feet high) on the cross bridge (Kessler Ave.) over the interstate highway I-65 in Indianapolis, Indiana. The video frames are from both incoming and outgoing traffics. The system was implemented on a dual Pentium 1.8G M laptop to measure the accuracy of the system, two criteria that are commonly used to evaluate performance in information retrieval are the precision rate and recall rates (18):

$$\text{precision rate} = \frac{\text{No. of correctly detected cars}}{\text{No. of detected cars}} \tag{2-10}$$

$$\text{recall rate} = \frac{\text{No. of correctly detected cars}}{\text{No. of cars}} \tag{2-11}$$

The precision rate measures the percentage of the correctly detected and counted cars within each video frames as opposed to detected cars, while the recall rate measures the percentage of correctly detected cars that actually a cars. In 3000 video frames for incoming traffic and 3000 video frames for outgoing traffic. There are 70 cars for outgoing traffic, and 61 cars for incoming traffic. For outgoing traffic, all 70 cars were correctly detected, but 6 cars have been counted twice. For incoming traffic, 60 cars were correctly detected, but 2 cars have been counted twice. The overall precision rate is 94.2%, and the recall rate is 99.2%. The experimental results demonstrate the effectiveness of our system.

Dynamic Vehicle Classification

To make the system to be flexible, the users are allowed to setup the camera at wide range of locations, heights, and angles. This created a great challenge in vehicle classification, where there is no baseline about what the size and projection of a typical vehicle could be. In the literature, researchers have used two approaches: using the parameters of the camera to accurately estimate the projection and the size of vehicle; or use neural network approach for the training.

However, both approaches would not work in this project. In the first approach, to accurately measure the parameters of the camera setting, the users need to have a lot of measurements of the setup, including the height from the camera to the ground, the road curvature, the tripod setup, the angle of the camera, the camera room ration, and the angle between the camera to the vehicle when it proceeds in the scene. All of these are not only taking time, but also may not be feasible. In the second approach, to use neural network, a lot of training would be necessary and the accuracy may not be high (18).

In this study, the Maximum-likelihood approach was utilized for vehicle classification.

(a) Review of the Maximum-likelihood Method. The maximum-likelihood estimation method has two advantages (19). First, it has very good convergence properties as the number of training samples increases. Second, it is very simple in implementation and gives firm estimation. Suppose that a collection of samples is separated according to class, the *c* data sets, $D_1,...,D_c$ can be determined with the samples in D_j having been drawn independently according to the probability law $p(\mathbf{x}\,|\,\omega_j)$. There are several cases. When the samples behavior is unknown, the worst scenario where samples are independent and identically distributed random variables (i.i.d), $p(\mathbf{x}\,|\,\omega_j)$ can be assumed, and is therefore determined uniquely by the value of a parameter vector $\boldsymbol{\theta}_j$.

Assume that the $p(\mathbf{x}\,|\,\omega_j)$ is Gaussian distribution: $p(\mathbf{x}\,|\,\omega_j) \sim N(\boldsymbol{\mu}_j, \Sigma_j)$, where $\boldsymbol{\mu}_j$ represents the mean vector of the distribution of $\boldsymbol{\theta}_j$, and Σ_j represents the variance vector of the distribution. And $\boldsymbol{\theta}_j$ consists of the components of $\boldsymbol{\mu}_j$ and Σ_j. Since $p(\mathbf{x}\,|\,\omega_j)$ is independent of $\boldsymbol{\theta}_j$, $p(\mathbf{x}\,|\,\omega_j)$ can be rewritten as $p(\mathbf{x}\,|\,\omega_j, \boldsymbol{\theta}_j)$. The goal is to use training samples to obtain good estimates for the unknown parameter vectors $\boldsymbol{\theta}_1,...,\boldsymbol{\theta}_c$. Suppose that D contains n samples $\mathbf{x}_1,...,\mathbf{x}_n$. Because the samples were drawn independently, the following equation is obtained.

$$p(D\,|\,\boldsymbol{\theta}) = \prod_{k=1}^{n} p(\mathbf{x}_k\,|\,\boldsymbol{\theta}). \qquad \text{(2-12)}$$

If $p(D\,|\,\boldsymbol{\theta})$ is well-behaved, differential function of $\boldsymbol{\theta}$, $\hat{\boldsymbol{\theta}}$ can be found by the standard methods of differential calculus. If the parameters to be estimated is p, let $\boldsymbol{\theta}$ denote the p-component vector $\boldsymbol{\theta} = (\theta_1,...,\theta_p)^t$, and $\nabla_{\boldsymbol{\theta}}$ be the gradient operator:

$$\nabla_{\boldsymbol{\theta}} \equiv \begin{bmatrix} \dfrac{\partial}{\partial \theta_{\mathbf{1}}} \\ \vdots \\ \dfrac{\partial}{\partial \theta_{\mathbf{p}}} \end{bmatrix} \qquad (2\text{-}13)$$

Defining $l(\boldsymbol{\theta})$ as the log-likelihood function yields the following equation:

$$l(\boldsymbol{\theta}) \equiv \ln\ p(D\,|\,\boldsymbol{\theta}) \qquad (2\text{-}14)$$

The estimated $\hat{\boldsymbol{\theta}}$ can be derived as:

$$\hat{\boldsymbol{\theta}} = \underset{\boldsymbol{\theta}}{\mathbf{arg\ max}}\ l(\boldsymbol{\theta}) \qquad (2\text{-}15)$$

where, the dependence on the data set D is implicit. Plot Eq. (2-12) into Eq. (2-14) yields the equations as follows:

$$l(\boldsymbol{\theta}) = \sum_{k=1}^{n} \ln\ p(\mathbf{x_k}\,|\,\boldsymbol{\theta}) \qquad (2\text{-}16)$$

$$\nabla_{\boldsymbol{\theta}} l(\boldsymbol{\theta}) = \sum_{k=1}^{n} \nabla_{\boldsymbol{\theta}} \ln\ p(\mathbf{x_k}\,|\,\boldsymbol{\theta}) \qquad (2\text{-}17)$$

Thus, a set of necessary conditions for the maximum-likelihood for $\boldsymbol{\theta}$ can be obtained from the set of p equations.

$$\nabla_{\boldsymbol{\theta}} l(\boldsymbol{\theta}) = 0 \qquad (2\text{-}18)$$

A solution $\hat{\boldsymbol{\theta}}$ to Eq. (2-18) could represent a true global maximum, a local maximum or minimum, or (rarely) an inflection point of $l(\boldsymbol{\theta})$. Therefore, it is important to check if the extreme occurs at a boundary of the parameter space, which might not be apparent from the solution. If all solutions are found, it is guaranteed that one represents the true maximum.

(b) Data Training. In this study, the sample training is necessary. More training data can help improve the recognition accuracy. However, it can take longer time. In a real-time setting, more training could mean loose more data.

In this study, a quick training method that can be performed as little as 2000 frames (about 1 minute) training was proposed. The users can also change the number of training frames according to their needs. When the unknown size vehicle passes by, the system will ask the users to input the vehicle class. And the system will use the maximum likelihood estimation method introduced in the section, Review of the Maximum-likelihood Method, to train the system. The value of this type of vehicle will be updated and listed in the software for the users to review.

Occasionally, the segmentation may not be correct due to the quality of the image. As a result, the trained result may not be correct. The proposed system allow the users to correct the numbers based their experience.

(c) Image Projection and Size Correction Using Projection Geometrics. When acquiring the image, due to the angle of the camera, the lane sizes are usually non-uniform in the image. The vehicles (3D objects) are projected into 2-D plane (images). Many researchers have tried to model the 3D objects from the 2D image. Some of them used multiple cameras, and some of them used quite complicated math functions. These approaches not only made the system unnecessarily complicated, but also have to have a lot of ideal assumption which would not work at all in real-life scenario.

Figure 2-19 gives a demonstration of how image acquisition process becomes the projection process. As a result, the center lanes tend to be wider than the side lanes in an image (if the camera is focused on the center lanes). Also, the road closer to the camera are usually much wider than the road further way. All these would affect the actual size of the vehicle in the image. For vehicles, the closer to the camera parts would look much bigger/wider than those of further way. It is important to properly project the data in the right plane.

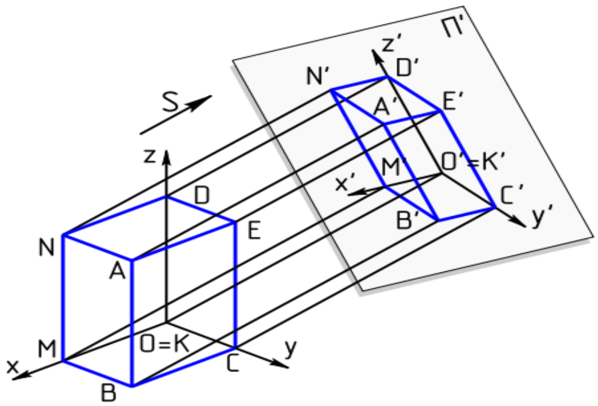

Figure 2-19 Demonstration of Object Projection from 3D to 2D (20)

In this study, the projective geometry method was used to project the vehicles into the corrected plane. The challenging of the projection is that the object may be locally deformed. And different locations of the same object may have their own projection metrics. In computer graphics, one of the most common matrices used for projection is 6=tuple, (left, right, bottom, top, near, far), which defines the clipping planes. These planes form a box with the minimum corner at (left, bottom, near), and the maximum corner at (right, top, far). The box is translated by:

$$P = \begin{bmatrix} \frac{2}{right-left} & 0 & 0 & -\frac{right+left}{right-left} \\ 0 & \frac{2}{top-bottom} & 0 & -\frac{top+bottom}{top-bottom} \\ 0 & 0 & \frac{2}{far-near} & -\frac{far+near}{far-near} \\ 0 & 0 & 0 & 1 \end{bmatrix} \quad (2\text{-}19)$$

It can also be given as a translation followed by a scaling of the form:

$$P = ST = \begin{bmatrix} \frac{2}{right-left} & 0 & 0 & 0 \\ 0 & \frac{2}{top-bottom} & 0 & 0 \\ 0 & 0 & \frac{2}{far-near} & 0 \\ 0 & 0 & 0 & 1 \end{bmatrix} \begin{bmatrix} 1 & 0 & 0 & -\frac{left+right}{2} \\ 0 & 1 & 0 & -\frac{top+bottom}{2} \\ 0 & 0 & 1 & -\frac{far+near}{2} \\ 0 & 0 & 0 & 1 \end{bmatrix} \quad (2\text{-}20)$$

However, in this study, it was unable to get the three dimensional parameters from the 2D image. It is ill-posed to model an 3D object by 2D image. Fortunately, only the size information from the vehicle is needed for classification purpose. In this study, instead of modeling the projection process as a 3D object to a 2D object, it was proposed to model the projection process as from 2D plane to another 2D plane. It was assumed that the original 2D plane has corrected ration of the vehicles in the lane, while the observed image was the projected result. Figure 2-20 demos our linear projection idea. In this way, it becomes a linear projective geometry question to estimate the correct vehicle sizes for classification. Here RP plane assumes to be the correct sized vehicle plane, pp plane is the observed image plane. Since it is from 2D to another 2D plane, the parameters can be easily and accurately estimated.

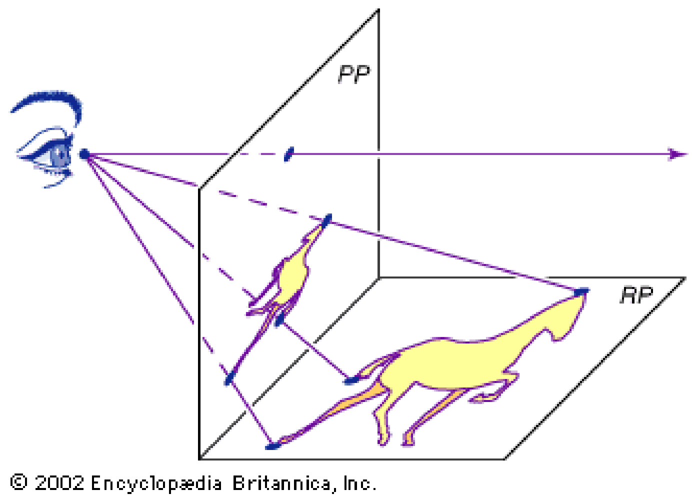

Figure 2-20 Linear Projective Geometry, Image from (21)

The following is a brief introduction of Projective Geometry.

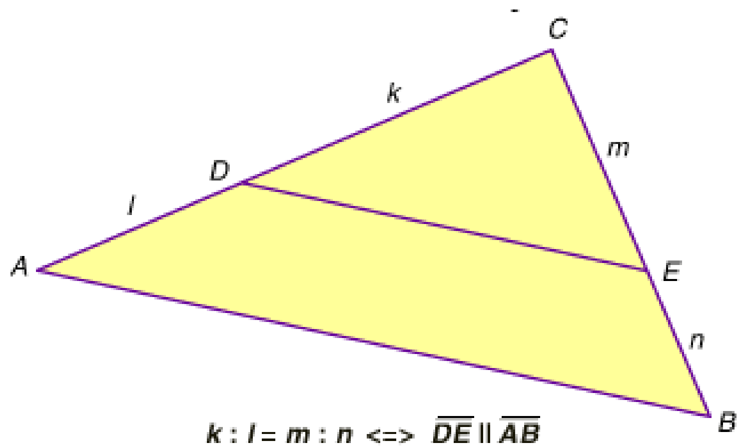

Figure 2-21 Fundamental Theorem of Similarity, Image from (21)

The fundamental theorem of similarity (Figure 2-21) is used in this project to vehicle projection transformation. In this theorem, it is a fact that for a triangle ABC, with line segment DE parallel to side AB:

$$CD/DA = CE/EB. \qquad (2\text{-}21)$$

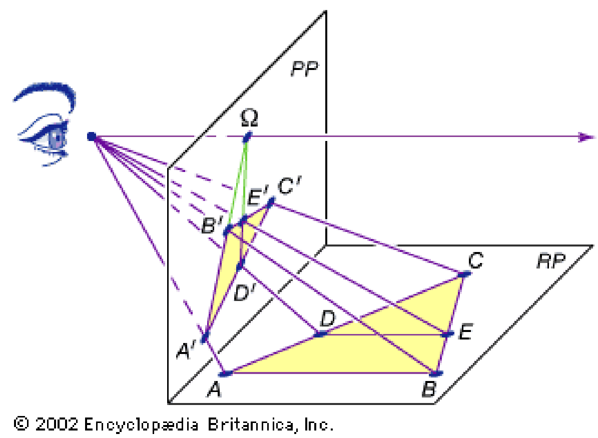

Figure 2-22 Parallel Lines in Projective Planes (Menelaus's Theorem), Image from (21)

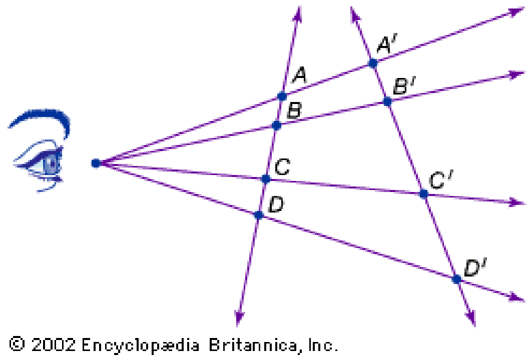

Figure 2-23 Cross Ratio, Image from (21)

Now in the plane situation (Figure 2-22), it is noted that A'B' and D'E' are not parallel; i.e. the angles are not preserved. From the point of view of the projection, the parallel lines AB and DE appear to converge at the horizon, or at infinity, whose project in the picture plane is labeled Ω. With the introduction of Ω, the projected figure corresponds to a theorem discovered by Menelaus:

$$C'D'/D'A' = C'E'/E'B' \cdot \Omega B'/\Omega A' \qquad (2\text{-}22)$$

The cross ratio given four distinct collinear points A, B, C, D (Figure 2-23), the cross ratio is defined as:

$$CRat(A,B,C,D) = AC/BC \cdot BD/AD \qquad (2\text{-}23)$$

Or

$$CRat(A,B,C,D) = AC/BC \cdot AD/BD \qquad (2\text{-}24)$$

Eq. (2-24) reveals the cross ratio as a ratio of ratios of distances. Pappus proved that the startling fact that the cross ratio was invariant, even though neither distance nor the ratio of distance is preserved under projection:

$$CRat(A,B,C,D) = CRat(A',B',C',D') \qquad (2\text{-}25)$$

In this project, Eq. (2-25) and Eq. (2-21) were used to correctly estimate the vehicle size in a corrected plane. Please note: this plane does not exist in the image, but it is mathematically used to correct the ratio of the vehicle.

Shadow Reduction

Shadows (Figure 2-24) are determined based on three criteria; average color of the cluster, cluster location relative to a cluster in an adjacent lane, and the shadow probability for that particular lane. A shadow is defined as an adjacent cluster whose average color is less than 105. For a given training period, the number of potential shadows is counted. Once the training period expires, and a potential shadow is detected, one of two clusters could potentially be the shadow. If both clusters are dark in color, the cluster with the higher probability is determined to be the shadow and is removed from the difference frame. Figure 2-25 provides the flow chart for the shadow detection algorithm.

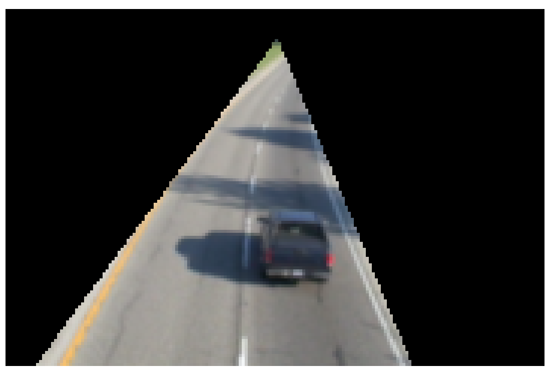

Figure 2-24 Example of a Video Frame with Shadow

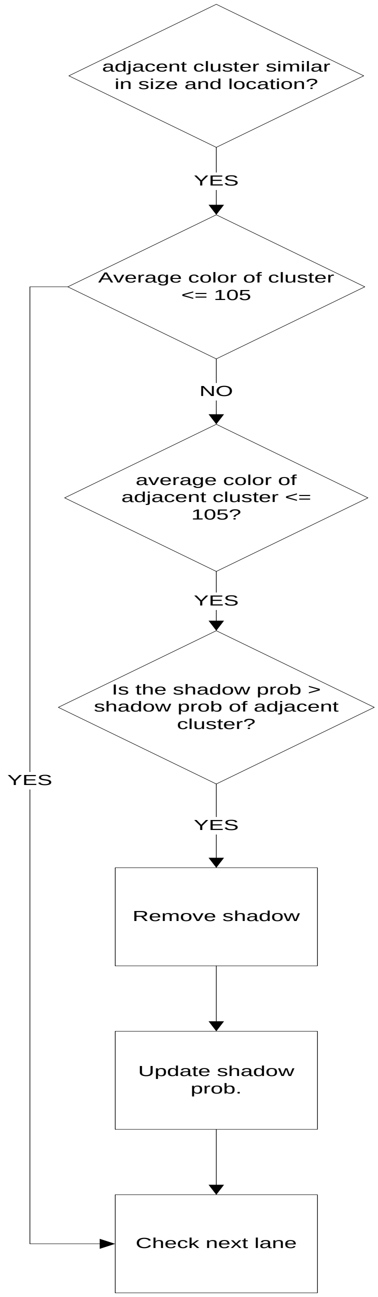

Figure 2-25 Shadow Removal Algorithm

As expected, the mean shift algorithm is too computationally expensive for a real-time system. As a trivial case, an example image was created with clearly defined boundaries. The mean shift clustering algorithm was successfully used to determine the boundaries, but took several seconds to process the trivial image. Although the results were favorable, such a large processing time makes the algorithm unusable for the vehicle tracking system. Figure 2-13 shows the results from mean shift segmentation where the colored circles are the original image and the clustered image is on the right. The different shades of gray represent different clusters.

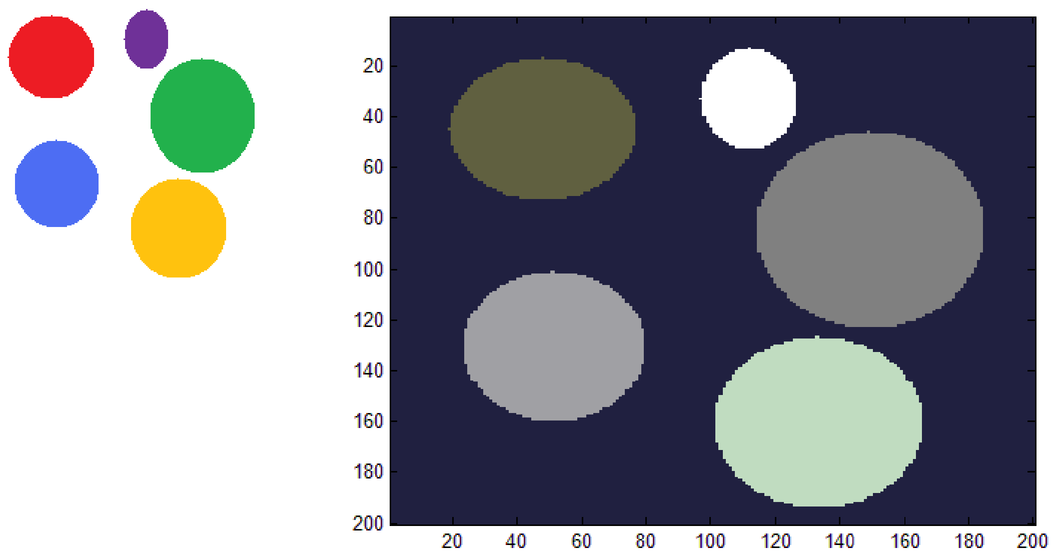

Figure 2-26 Mean Shift Clustering Results

The adaptive thresholding provides a fast segmentation, but detected too many features of the background as foreground features. The added computational time to remove the unwanted background features eliminates the adaptive thresholding as a candidate for this system. This segmentation technique would be better suited for non real-time applications with more clearly defined boundaries between the foreground and background features. Figure 2-14 shows an example of a frame that has been segmented using adaptive thresholding.

The difference frame method produced better results than the adaptive thresholding with a comparable amount of computational time. A problem arises when trying to connect clusters in the same lane. The algorithm previously outlined would sometimes connect clusters which do not belong to the same vehicle. In a group of 243 images, 27 were found to be incorrectly segmented due to the inaccurate cluster connections (error rate of 11%). The average processing time for the difference method, using 243 images, was found to be 11 ms, which is sufficient for real-time processing, but the error rate of 11% is too high. Figure 2-15 shows the incorrect connections between clusters while Figure 2-16 gives an example of a correct connection using the difference frame method.

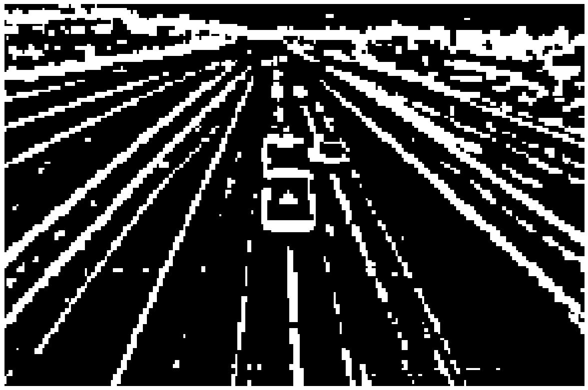

Figure 2-14 Adaptive Thresholding Result

Figure 2-15 Incorrect Cluster Connection

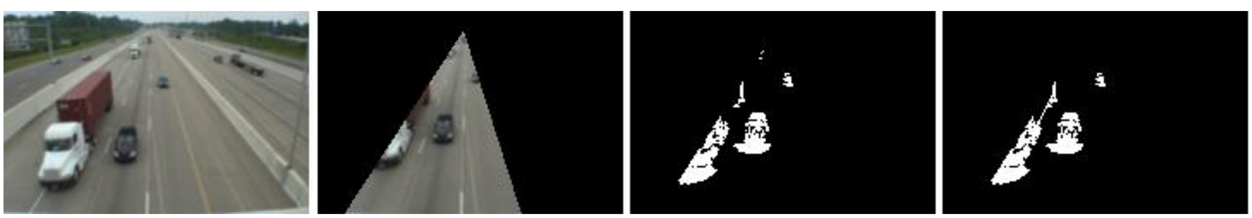

Figure 2-16 Correct Cluster Connection

The shadow detection and removal algorithm has provided promising results. Of the 154 images tested, only 6 shadows were left unresolved, giving a preliminary success rate of 96%, with an average computational time of 13 ms. Although the results are promising, the tests conducted were with still images and further testing must be completed using the real-time system. Also, the only test data available included a two lane road and for completeness, the algorithm needs to be tested with three or more lanes. Figure 2-17 illustrates results of a successful shadow removal scenario.

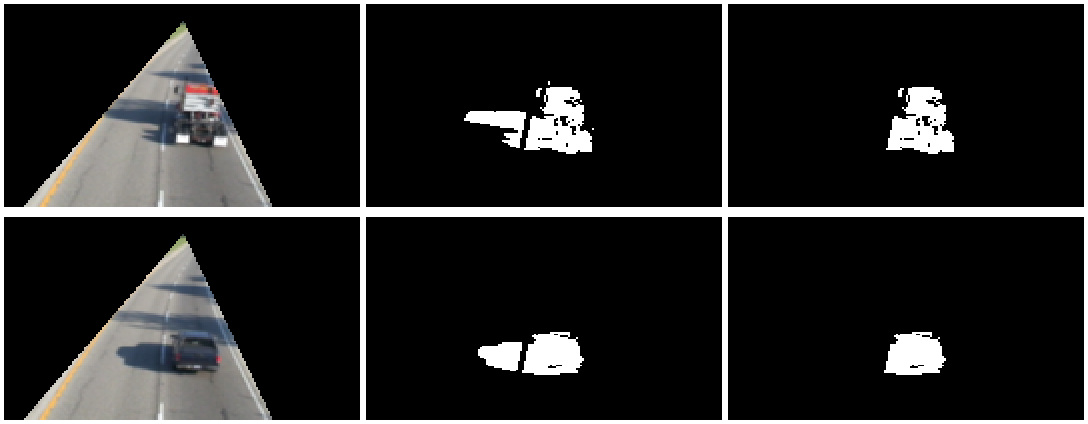

Figure 2-17 Results from the Shadow Detection and Removal Algorithm

In summary, several segmentation methods were studied in an attempt to find an alternative method for a real-time vehicle counting and classification system. The mean shift clustering algorithm has shown promising accuracy, but is computationally expensive and is therefore not best suited for this system. The adaptive thresholding technique is fast, but the segmentation results are highly inaccurate. The difference frame method has the best combination of accuracy and computation time, but requires the use of an algorithm to connect neighboring clusters. The connection algorithm provides inaccuracies in the final segmentation by connecting clusters which do not belong to the same vehicle. In the end, it is determined that the current segmentation system provides a better balance of accuracy and speed as compared to the three methods attempted. In addition to investigating segmentation techniques, an algorithm was developed to detect and remove unwanted shadows in the real-time system. The preliminary results show promise and thus prompting the integration into the real-time system.

The Video Image Processing System

In order to validate the unclassified vehicle data associated with WIM vehicle classification using automatic vehicle classification with video, a video image processing system as shown in

Figure 2-18 was developed using the dynamic content-based vehicle tracking and traffic monitoring algorithms. In this study, a camcorder, DCR-SR100 30GB Handycam® CamcorderDCR-SR100, was used to record the video vehicle data onto a VHS tape at the selected WIM sites.

The step-by-step instruction to use this system is provided in Appendix I.

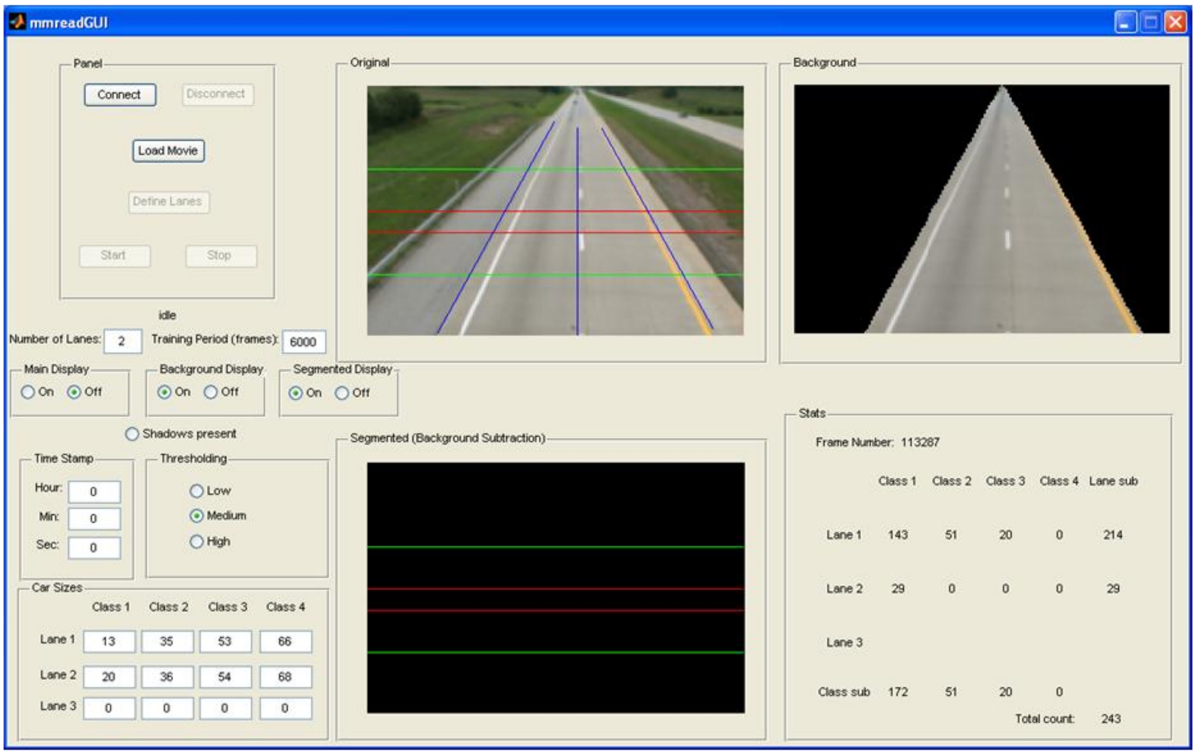

Figure 2-18 Full View of the Software

Chapter 3

VALIDATION OF WIM VEHICLE CLASSIFICATION DATA USING VIDEO COUNTS

WIM Vehicle Classification Data

Potential Errors Associated with WIM vehicle Classification

For vehicle classification at a WIM site, sensors are placed in pavement to detect the arrival of vehicle axles and generate correspondent signals. The signals are processed to determine vehicle sizes and axle configurations to identify vehicle classes with a specific algorithm. Therefore, the accuracy of vehicle classification depends on the sensitivity of sensors, environments, and road conditions such as the number of lanes and traffic characteristics. Two types of errors may arise in WIM vehicle classifications. First, data are missing from a particular WIM lane or all WIM lanes (22). Data missing from all lanes is probably due to a system failure. However, data missing from a particular lane is probably due to a lane closure or a sensor malfunction.

The second type of vehicle classification errors is that vehicles may not be classified. When a vehicle executes lane changing on a multi-lane road, it is possible that only part of the vehicle crosses the sensors. Vehicles may also accelerate or decelerate over the sensor, resulting in a speed variation over the sensor. Additionally, different sensors may use different classification algorithms that are not a pure science. As a result, errors may be involved in vehicle classifications. Because missing data can be easily identified from WIM reports and because vehicle unclassification may be involved at every WIM site, the validation of WIM classification focused on vehicle unclassification.

WIM Classification Data

There are forty seven WIM sites on the highways under INTOT jurisdiction, thirty one sites on interstate highways, and sixteen sites on US highways and State roads. The selection of WIM sites for examining vehicle classifications was made mainly by taking into account those factors affecting vehicle classifications, in particular number of lanes, traffic volume, and truck volume. In addition, the ground conditions at the WIM sites should be suitable for safely setting up a camera tripod to record quality video tapes of traffic at a certain angle. Presented in Table 3-1 is the data on vehicle counts and unclassified vehicles at the selected eighteen WIM sites.

Table 3-1 WIM Vehicle Classification Data at Selected WIM Sites

WIM Site Info				Traffic Counts						Unclass. (%)
Site	Road	Dir.	Lanes	Vehicle Category					Total Counts	
				1	2	3	4	Unclass.		
2000	I69	NB	2	603	56	190	5	49	903	13.3
2000	I69	SB	2	457	197	16	0	311	981	50.6
2300	I69	SB	2	397	316	279	4	22	1018	4.2
3400	I65	NB	3	1734	208	142	6	333	2423	40.3
3400	I65	SB	3	1846	206	278	14	82	2426	10.1
3510	I465	NB	6	3709	358	410	7	142	4626	34.5
3530	I465	SB	6	4626	252	309	10	212	5409	23.5
3600	I70	EB	2	648	70	264	15	95	1092	16.3
3600	I70	WB	2	822	36	208	24	52	1142	8.6
3700	I70	EB	2	667	73	312	23	20	1095	3.8
3700	I70	WB	2	706	177	329	11	32	1255	4.9
4000	I80/94	EB	4	1273	160	861	9	67	2370	7.6
4000	I80/94	WB	4	1023	133	376	5	883	2420	87.5
4100	I65	NB	2	814	102	160	1	313	1390	44.9
4100	I65	SB	2	912	59	316	13	14	1314	2.1
4200	I65	NB	3	2714	121	371	7	53	3266	4.8
4210	I65	SB	3	2864	149	341	11	59	3424	5.3
4400	I80/94	EB	3	2042	176	901	18	57	3194	5.6
4400	I80/94	WB	3	1836	178	868	9	276	3167	23.2
5300	I74	EB	2	1129	130	148	4	16	1427	2.3
5300	I74	WB	2	549	43	95	0	7	694	2.7
5400	I64	EB	2	778	59	161	6	11	1015	2.1
5400	I64	WB	2	1195	103	185	2	25	1510	3.1
5500	I65	NB	3	1156	165	364	9	95	1789	15.8
5510	I65	SB	3	1500	143	359	15	48	2065	6.9
6100	I64	EB	2	504	39	164	2	12	721	3.0
6100	I64	WB	2	538	42	187	2	15	784	4.0
6200	I64	EB	2	520	40	128	2	21	711	5.4

Video Vehicle Classification Data

Video Traffic Data Acquisition

Two main concerns may arise during video traffic data recording. In reality, the workplace is a temporary roadside work zone involving people and equipment. While most overpass bridges are on low volume roads, temporary traffic control devices to delineate the workplace. As a general rule of thumb (23, 24), it is necessary to ensure all people, recording system, and vehicles are visible to motorists. Equipment should not be placed behind grades or curves where sight distance may not be sufficient. The second concern is the quality of data. In order to record the vehicle data in the whole site, the camcorder should be placed above the middle of the driveway and oriented down at 30~45 degrees (Figure 3-1). Light condition requires the clear view of the scene and no long shadow of the vehicle. The best recording time period is 11am-2pm. To ensure the camcorder's tolerance, temperature should be 32 to 95 ^{o}F.

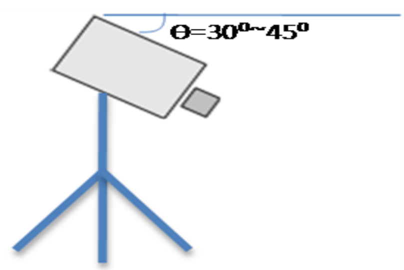

Figure 3-1 Camcorder Setting

Video Classification Data

In this study, Video traffic data was collected in July-August, 2007. The video tapes of traffic were recorded using a camcorder, DCR-SR100 30GB Handycam® CamcorderDCR-SR100. The camera tripod was usually set up on overpass bridges or places with a relatively high elevation above the road. During traffic data recording, the camera was pointed to the back end of the traffic flow downstream so as to avoid possible intrusion to motorists. At most selected WIM site, the traffic flows in both directions were recorded. Due to the limitation of the video tape length, only one hour traffic data was recorded in each direction. Table 3-2 shows the vehicle classification data collected at twenty WIM sites.

Table 3-2 Video Vehicle Classification Data at WIM Sites

WIM Sites				Vehicle Category				Total Counts
Site	Road	Dir.	Lanes	1	2	3	4	
1100	I-65	SB	2	436	159	187	30	812
1100	I-65	NB	2	939	167	177	0	1283
1300	I-70	WB	2	1090	80	368	29	1567
1300	I-70	EB	2	565	80	212	23	880
2000	I-69	NB	2	530	116	203	45	894
2000	I-69	SB	2	637	50	218	13	918
3400	I-65	NB	3	1630	143	286	19	2078
3400	I-65	SB	1	500	19	6	0	525
3400	I-65	SB	3	1818	189	289	12	2308
3600	I-70	EB	2	410	49	178	11	648
3600	I-70	WB	2	810	76	240	24	1150
3700	I-70	EB	2	803	99	290	12	1204
3700	I-70	WB	2	807	69	260	7	1143
4000	I-80/94	EB	3	1570	188	1050	17	2825
4010	I-80/94	WB	3	1171	123	1100	20	2414
4100	I-65	SB	2	732	88	180	23	1023
4100	I-65	NB	2	707	49	350	6	1112
4200	I-65	NB	3	2106	120	366	12	2604
4210	I-65	SB	3	2300	140	295	12	2747
4400	I-80/94	WB	3	1860	148	928	16	2952
4400	I-80/94	EB	3	1730	262	754	168	2914
4700	SR-49	NB	2	683	47	78	3	811
4700	SR-49	SB	2	1000	111	72	9	1192
5100	I-65	NB	2	952	81	226	5	1264
5100	I-65	SB	2	657	233	99	103	1092
5300	I-74	WB	2	458	21	165	9	653
5300	I-74	EB	2	460	39	158	1	658
5400	I-64	EB	2	632	107	57	9	805
5400	I-64	WB	2	1140	176	130	6	1452
5500	I-65	NB	4	1178	171	230	40	1619
5510	I-65	SB	4	2284	354	297	100	3035
6100	I-64	EB	2	470	48	141	2	661
6100	I-64	WB	2	545	40	176	3	764
6200	I-64	EB	2	505	36	152	2	695
6200	I-64	WB	2	450	48	153	7	658

Data Analysis

<u>Tolerance for Unclassified Vehicle Counts</u>

Three observations can be made by careful inspection of the data in Table 3-1. First, at WIM Site 4000, the unclassified vehicles reached 87.5% of total vehicle counts in westbound. This is extremely high and might be due to a sensor failure. This site consists of four lanes in each direction. Further examination of the WIM report indicated that the data was missed for the left lane in both directions. However, the adjacent lane in west bound did not exhibit an increased vehicle counts. This implies that the missing data was probably due to a sensor malfunction. Other WIM sites that might experience sensor problems are those where unclassified vehicles exceed 30% of the total vehicle counts. The second observation is that traffic volume might also contribute to the vehicle unclassification issue. Plotted in Figure 3-2 are the variations of unclassified vehicles (%) with vehicle counts. Notice that the data for those WIM site that might experience sensor malfunctions was not included.

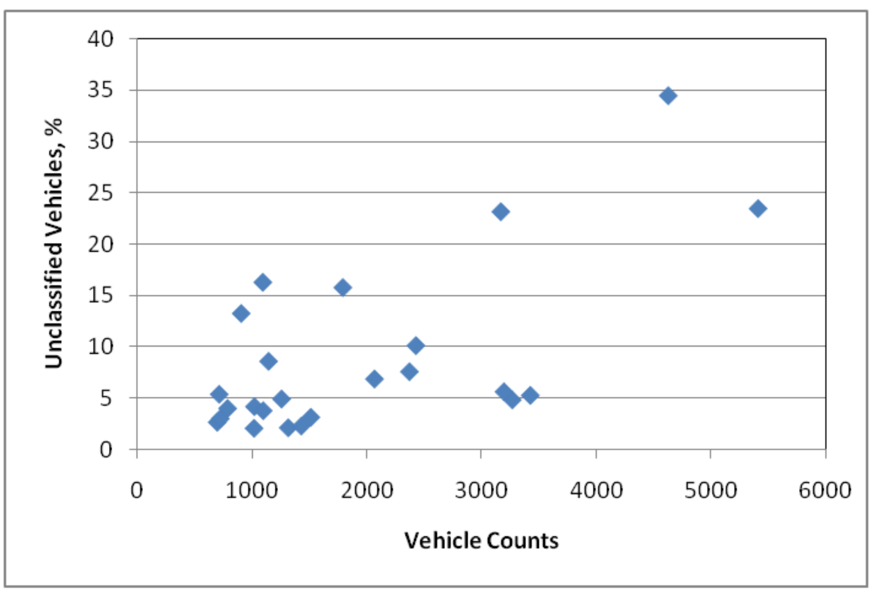

Figure 3-2 Variations of Unclassified Vehicles with Traffic Volume

It is shown that while most WIM sites witnessed a traffic volume varying from 600 to 3000 vehicles per hour, it appears that the percentage of unclassified vehicles increases as vehicle counts increases. In reality, it was hypothesized that as traffic volume increases, the interaction between vehicles increases and more vehicles may execute lane changing and passing. The third observation is that in general, the percentage of unclassified vehicles increases as the number of travel lanes increases at the WIM site as shown in Figure 3-3. This is probably because at a WIM site with more travel lanes, the possibility for vehicles to execute lane changing or passing increases. Therefore, more vehicles may occupy the two adjacent lanes or change speeds at sensors, which leads to greater percentages of unclassified vehicles.

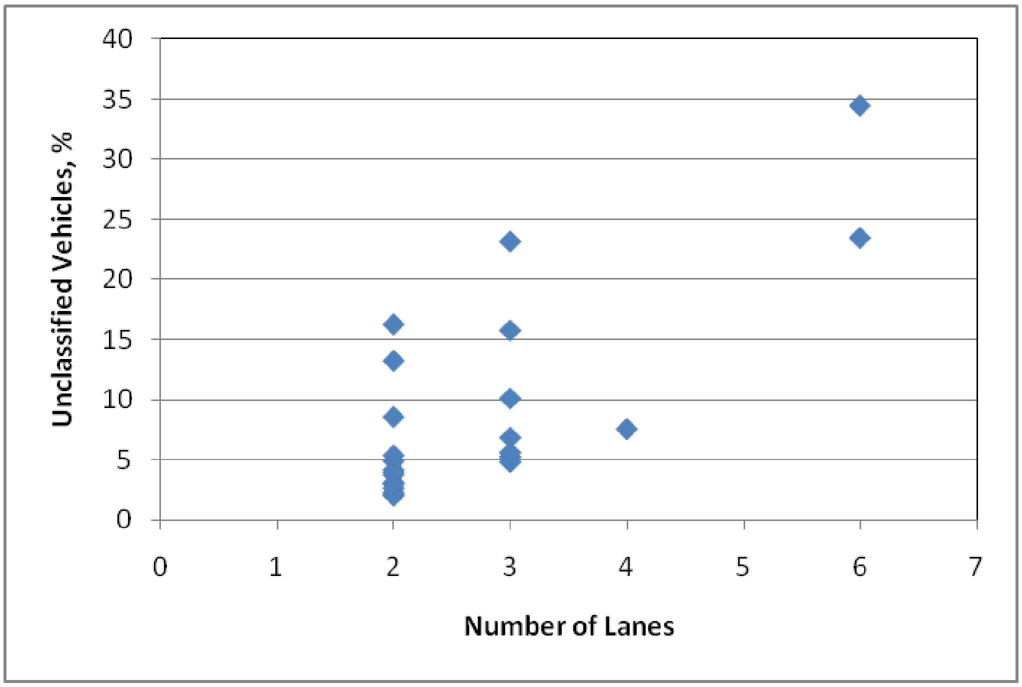

Figure 3-3 Variations of Unclassified Vehicles with Number of Lanes

This project examined the vehicle counts and classification data lane by lane and eliminated those WIM sites with suspicious vehicle count data. As shown in Table 3-3 are the summaries of the percentages of unclassified vehicles in each WIM lane with verified data. Since the WIM sites utilize various sensors and the number of lanes varies from site to site, it is difficult to determine specific bounds for estimating the percentage of unclassified vehicles at each WIM site. Based on the unclassified vehicle data in Table 3-3, however, it appears that unacceptable errors may be involved in the vehicle classification when the percentage of unclassified vehicles for a single lane exceeds 4% of the total vehicle counts in that lane at a confidence level of 95%. In other words, it is not acceptable when the percentage of unclassified vehicles exceeds 4% for a single lane.

Table 3-3 Summaries of Percentages of Unclassified Vehicles for Each WIM Lane

WIM Site	Lane ID	Unclass. (%)	WIM Site	Lane ID	Unclass. (%)	WIM Site	Lane ID	Unclass. (%)
2000	NB-#1	2.56	3600	WB-#3	5.34	4400	WB-#2	18.36
2000	NB-#2	10.69	3600	WB-#4	3.25	4400	WB-#3	1.91
2000	SB-#4	5.07	3700	EB-#1	1.72	5300	EB-#1	0.78
2300	SB-#1	2.38	3700	EB-#2	2.06	5300	EB-#2	1.51
2300	SB-#2	1.8	3700	WB-#3	3.03	5300	WB-#3	0.22
3400	NB-#2	2.51	3700	WB-#4	1.89	5300	WB-#4	2.44
3400	NB-#3	0.56	4000	EB-#1	1.34	5400	EB-#1	1.19
3400	SB-#4	5.62	4000	EB-#2	2.49	5400	EB-#2	0.88
3400	SB-#5	2.19	4000	EB-#3	3.75	5400	WB-#3	2.24
3400	SB-#6	2.31	4010	WB-#5	2.71	5400	WB-#4	0.9
3500	NB-#1	21.19	4010	WB-#6	3.35	5500	NB-#1	5.18
3500	NB-#2	2.92	4100	NB-#2	0.58	5500	NB-#2	6.35
3500	NB-#3	3.42	4100	SB-#1	1.15	5500	NB-#3	4.24
3510	NB-#4	2.23	4100	SB-#2	0.97	5510	SB-#4	1.33
3510	NB-#5	2.06	4200	NB-#1	1.05	5510	SB-#5	3.35
3510	NB-#6	2.63	4200	NB-#2	2.12	5510	SB-#6	2.19
3520	SB-#1	6.28	4200	NB-#3	1.67	6100	EB-#1	1.8
3520	SB-#2	3.42	4210	SB-#4	1.35	6100	EB-#2	1.2
3520	SB-#3	3.66	4210	SB-#5	2.87	6100	WB-#3	1.8
3530	SB-#4	3.98	4210	SB-#6	1.05	6100	WB-#4	2.2
3530	SB-#5	3.61	4400	EB-#4	2.6	6200	EB-#1	3.11
3530	SB-#6	2.51	4400	EB-#5	2.78	6200	EB-#2	2.27
3600	EB-#1	11.09	4400	EB-#6	0.25			
3600	EB-#2	5.19	4400	WB-#1	2.89			

Adjustment of Unclassified Vehicle Counts

In order to identify the compositions of unclassified vehicle counts at WIM sites, the video vehicle counts presented in Table 3-2 are employed to validate the WIM vehicle counts. Comparison can be made on the total WIM vehicle counts and the total video vehicle counts in each direction at the WIM site as illustrated in Figure 3-4. In general, both the WIM vehicle counts and the video vehicle counts follow a similar trend. However, great discrepancies can be observed at some WIM sites, such as Sites 4200, 4210, 5510 SB, and 5300 WB. There are two possible contributing factors. First, it is very difficult to exactly match the time period for WIM vehicle counting to the time period for video vehicle counting. Any discrepancy between counting time periods may lead to a large discrepancy between vehicle counts. Second, errors may be involved in the unclassified vehicle count. It is possible that two or more vehicles might be counted as one unclassified vehicle.

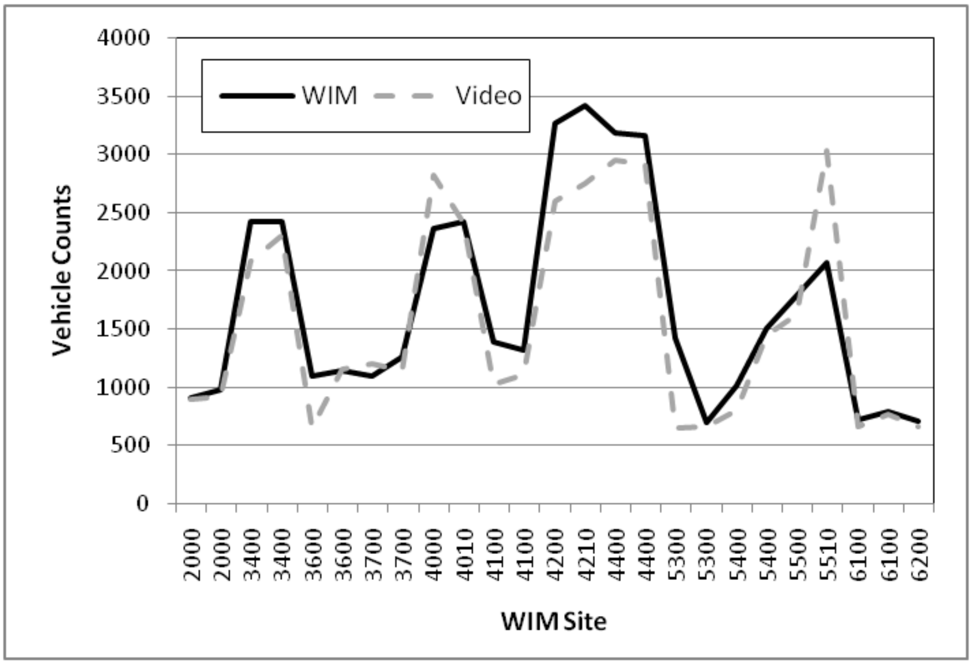

Figure 3-4 Comparison of WIM and Video Vehicle Counts

Therefore, the validation of unclassified vehicle counts was made by comparing the vehicle category distributions in WIM and video vehicle counts, rather than the vehicle counts. The vehicle category distribution is defined as the percentage of each vehicle category. Presented in Table 3-4 are the vehicle category distributions calculated from both the WIM and video vehicle counts. Category 1, i.e., passenger cars, accounts for the greatest percentage of the total vehicle counts, followed by Category 3, i.e., single tractor trailers, which accounts for up to 37% of the total vehicle counts. Single unit trucks are the third largest category and account for 10% at most WIM sites. Multi-trailer trucks under Category 4 account for the least percentage of the total vehicle counts, which is less than 3% at most WIM sites.

Table 3-4 Comparison of Vehicle Category Distributions

WIM Site Information				WIM Vehicle Category Distribution						Video Vehicle category Distribution				
Site	Road	Dir.	Lanes	1	2	3	4	Unclass.	Sum	1	2	3	4	Sum
2000	I69	NB	2	66.8	6.2	21.0	0.6	5.4	903	59.3	13.0	22.7	5.0	894
2000	I69	SB	2	46.6	20.1	1.6	0.0	31.7	981	69.4	5.4	23.7	1.4	918
3400	I65	NB	3	71.6	8.6	5.9	0.2	13.7	2423	78.4	6.9	13.8	0.9	2078
3400	I65	SB	3	76.1	8.5	11.5	0.6	3.4	2426	78.8	8.2	12.5	0.5	2308
3600	I70	EB	2	59.3	6.4	24.2	1.4	8.7	1092	63.3	7.6	27.5	1.7	648
3600	I70	WB	2	72.0	3.2	18.2	2.1	4.6	1142	70.4	6.6	20.9	2.1	1150
3700	I70	EB	2	60.9	6.7	28.5	2.1	1.8	1095	66.7	8.2	24.1	1.0	1204
3700	I70	WB	2	56.3	14.1	26.2	0.9	2.5	1255	70.6	6.0	22.7	0.6	1143
4000	I80/94	EB	4	53.7	6.8	36.3	0.4	2.8	2370	55.6	6.7	37.2	0.6	2825
4000	I80/94	WB	4	42.3	5.5	15.5	0.2	36.5	2420	48.5	5.1	45.6	0.8	2414
4100	I65	NB	2	58.6	7.3	11.5	0.1	22.5	1390	71.6	8.6	17.6	2.2	1023
4100	I65	SB	2	69.4	4.5	24.0	1.0	1.1	1314	63.6	4.4	31.5	0.5	1112
4200	I65	NB	3	83.1	3.7	11.4	0.2	1.6	3266	80.9	4.6	14.1	0.5	2604
4210	I65	SB	3	83.6	4.4	10.0	0.3	1.7	3424	83.7	5.1	10.7	0.4	2747
4400	I80/94	EB	3	63.9	5.5	28.2	0.6	1.8	3194	63.0	5.0	31.4	0.5	2952
4400	I80/94	WB	3	58.0	5.6	27.4	0.3	8.7	3167	59.4	9.0	25.9	5.8	2914
5300	I74	EB	2	79.1	9.1	10.4	0.3	1.1	1427	70.1	3.2	25.3	1.4	653
5300	I74	WB	2	79.1	6.2	13.7	0.0	1.0	694	69.9	5.9	24.0	0.2	658
5400	I64	EB	2	76.7	5.8	15.9	0.6	1.1	1015	78.5	13.3	7.1	1.1	805
5400	I64	WB	2	79.1	6.8	12.3	0.1	1.7	1510	78.5	12.1	9.0	0.4	1452
5500	I65	NB	3	64.6	9.2	20.3	0.5	5.3	1789	72.8	10.6	14.2	2.5	1619
5510	I65	SB	3	72.6	6.9	17.4	0.7	2.3	2065	75.3	11.7	9.8	3.3	3035
6100	I64	EB	2	69.9	5.4	22.7	0.3	1.7	721	71.1	7.3	21.3	0.3	661
6100	I64	WB	2	68.6	5.4	23.9	0.3	1.9	784	71.3	5.2	23.0	0.4	764
6200	I64	EB	2	73.1	5.6	18.0	0.3	3.0	711	72.7	5.2	21.9	0.3	658

The concerns on the unclassified vehicle counts have been raised by some researchers (25). Since the vehicle classification data has been widely used by transportation agencies, the importance of the work on making corrections on the unclassified vehicle counts can never be overestimated. It is shown that in Table 3-4, the greatest discrepancy between the WIM and video vehicle category distributions arose from Category 3, followed by Category 1 regardless of the number of lanes. This implies that the unclassified vehicles mainly involved single tractor trailers and passenger cars. The least discrepancy was observed for Category 2, which indicates that single unit trucks were most likely classified. While traffic volume and lane number are the two main contributing factors, it is unrealistic to predict the unclassified vehicles in terms of traffic volume and lane number at this time. However, the adjustment factors in Table 3-5 can be utilized to allocate the unclassified vehicles when it is needed. These factors are determined from the data in Table 3-4 and represent the percentages of the unclassified vehicles for the four vehicle categories, respectively.

Table 3-5 Adjustment Factors of Unclassified Vehicles

Vehicle Category	1	2	3	4
Adjustment Factors, %	35.0	5.0	48.0	12.0

Chapter 4

EVALUATION OF TIRTL'S FIELD PERFORMANCE

The TIRTL Vehicle Data Collection

One TIRTL system was installed to collect vehicle count and classification data by this study as shown in Figure 4-1. The installation site is located at milepost 177.43 on I-65 in Lafayette, Indiana, and is approximately 1.49 miles north of a weigh-in-motion (WIM) site on I-65. No any access exists between the TIRTL site and the WIM site. Figure 4-2 shows a graphical illustration of the locations of the TIRTL and WIM sites. There are four lanes at this site, two in each direction. The installation of TIRTL was fully completed in April, 2008. The transmitter is placed southbound and the receiver northbound. Both the transmitter and receiver are placed on a wood pole (see Figure 4-1), respectively, so as to avoid possible blocking of the light beam pathways by ground grasses or other obstacles in the median. The lane configuration at the TIRTL site is shown in Figure 4-3. The driving and passing lanes in the northbound are designated as Lane 1 and Lane 2 with negatively signed velocities, respectively. In the southbound, the driving and passing lanes are designated as Lane 4 and Lane 3 with positively signed velocities, respectively.

Figure 4-1 TIRTL System Installed on I-65 in Lafayette, IN

Figure 4-2 Graphical Illustration of TIRTL and WIM Sites

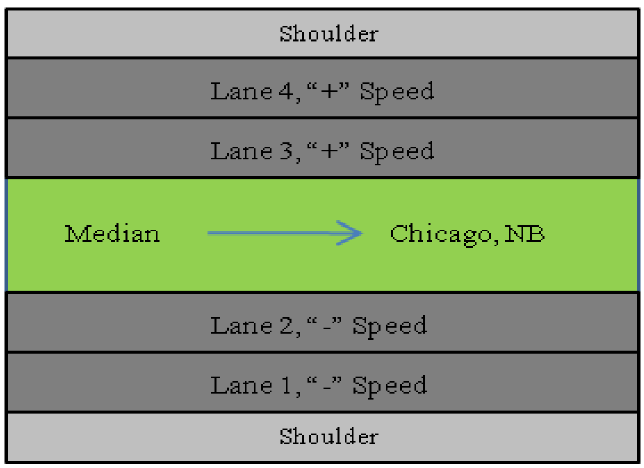

Figure 4-3 Lane Configuration

Three main files, including vehicle log file, system log file, and alarm log file can be downloaded with point to point protocol connection. The vehicle log file records vehicle data, including date, time, lane, velocity, and class number, axle count, wheel base, and class name. The vehicle classification is based on the so-called "Scheme F", in which, vehicles are classified into 15 categories. Categories 1 to 13 are as defined in Figure 2-1 in Chapter 2. Category 14 includes the special vehicles defined by DOT personnel. Category 15 includes those vehicles which do not confirm to the classification criteria for Class 1 through Class 14. The system log file is used to record all activities, including internal maintenance and development support.

The alarm log data includes date, time, alarm name, and channels. There are three main types of alarm, such as Beams Blocked, Beam Levels Degraded, and Beams Not Aligned. "Beams Blocked" simply indicates the beams are totally blocked due probably to an obstruction such as a vehicle parked front of the TIRTL system. "Beam Levels Degraded" implies that the generated bema light may experience the loss of lumens due to surrounding factors such as fog. If this occurs, however, the system may still perform well. "Beams Not Aligned" indicates that the beams are not traveling directly between the transmitter and receiver. This may occur during set up, and may also occur if the system cabinet is twisted.

Validation of TIRTL Data Accuracy by Manual Vehicle Counts

This study employed a manual vehicle count to validate the accuracy of the TIRTL vehicle classification data since the manual count usually represents the baseline in many circumstances. The manual vehicle count was conducted in the northbound direction on the Swisher Road overpass bridge that is located immediately upstream of the TIRTL site on November 2, 2009. It was clear, sunny. In order to reduce possible errors, the manual vehicle counting was made by two persons, one person for the passing lane and the other for the driving lane. Since the traffic volume was relatively high, the manual vehicle counting was made for one hour (9:10 am–10:10 am) in terms of four vehicle categories as defined in Table 2-1. Table 4-1 shows the detailed manual and TIRTL vehicle counts.

Table 4-1 Comparison of Manual and TIRTL Vehicle Counts

Vehicle Category	**Manual Count**		**TIRTLE Count**		**P. E.**	
	Driving Lane	Passing Lane	Driving Lane	Passing Lane	Driving Lane	Passing Lane
1	291	241	295	240	1.4%	0.4%
2	38	1	32	0	15.8%	100.0%
3	237	38	244	36	3.0%	5.3%
4	10	1	9	1	10.0%	0%
Sub-Total	576	281	580	277	0.7	1.42
Total	857		857		0%	

In order to measure the accuracy of the TIRTL vehicle count, the percent error used elsewhere (26) is employed by this study to quantify the potential errors associated with the TIRTL vehicle count. The calculation of the percent error depends on the baseline vehicle count. In this case, the percent error is computed as follows:

(4-1)

where, P.E. is the percent error, the baseline count represents the manual vehicle count, and the observed count represents the TIRTL vehicle count.

However, special care should be exercised when interpreting the percent errors, in particular if the baseline count is low. This is because the percent error represents a relative error. When the baseline count such as the manual count in Equation (4-1) is low, the calculated percent error may be very high. As a result, the performance of the traffic counter may be exaggerated. It is shown that the percent error for the total vehicle count in these two lanes is 0% and both the total manual vehicle count and the total TIRTL vehicle count are 857 vehicles, respectively. The percent error for the sub-total vehicle count in each lane is 0.7% for the driving lane and 1.4% for the passing lane. Apparently, the total TIRTL vehicle counts agree extremely well with the total manual vehicle count. For vehicle category count (or classification count), the percent error for Category 2 in the passing lane is 100% and 0% for Category 4 in the passing lane. However, this should be ignored simply because the baseline count, i.e., the manual count, is only one.

A more meaningful comparison should focus on Category 1 and Category 3 that account for approximately 94% of the total traffic volume. As demonstrated in Table 4-1, the percent error for Category 1 is 0.4% in the passing lane and 1.4% in the driving lane. For category 3, the percent error is 3.0% in the driving lane and 5.3% in the passing lane. The TIRTL vehicle category count agrees well with the manual vehicle category count for both Category 1 and Category 3. It was observed that during manual vehicle counting, the errors might arise due to two main factors. First, some vehicles executed lane-changing before arriving at the TIRTL site. Second, pick-up trucks towing trailers might be misclassified. The percent error for Category 3 is greater than that for Category 1. This implies that for TIRTL, the accuracy of vehicle classification for passenger cars is better that that for tractor trailers. This is similar to the finding for the vehicle classification by WIM as shown in Table 3-5.

Comparison of TIRTL and WIM Vehicle Counts

The Accuracy of WIM Vehicle Counts

In many circumstances, it is extremely labor intensive or even impractical to conduct manual vehicle counting, in particular on multi-lane interstate highways with high traffic volumes, in adverse weathers or for long duration counting. Therefore, the WIM vehicle classification data collected at the WIM site as shown in Figure 4-2 was employed to further evaluate the TIRTL performance. The requirements for WIM performance can be found elsewhere (27). In this study, video vehicle counts were used to double check the accuracy of the WIM vehicle counts. As tabulated in Table 4-2 are the Video and WIM vehicle counts made on November 21, 2008. The weather was clear.

Table 4-2 Comparison of Video and WIM Vehicle Counts

Vehicle Category	Video Count		WIM Count		P. E.	
	NB	SB	NB	SB	NB	SB
0	-	-	12	73	-	-
1	829	984	787	843	5.1%	14.3%
2	56	69	44	159	21.4%	130.4%
3	360	309	370	265	2.8%	14.2%
4	20	13	21	7	5.0%	46.2%
Total	1265	1375	1234	1347	2.5%	2.0%

The vehicle counts were made on the Swisher Road overpass bridge during a duration of one hour from 11:13am to 12:13pm in the northbound, and from 13:03pm to 14:03pm in the southbound. Since the Video and WIM sites are approximately one and half miles apart, Table 4-2 presents the total vehicle counts in direction instead of each individual lane because of the possible lane changing by vehicles between the Video and WIM sites. Category 0 represents the unclassified vehicles. It is shown that the total Video and WIM vehicle counts agree very well in both directions. The percent error is 2.5% in the northbound and 2.0% in the southbound. The percent errors for

Category 2 and Category 4 are very large. However, the vehicles in these two categories account only for about 6% of the total vehicles. This may not affect the overall performance of WIM vehicle classification very much.

TIRTL and WIM Daily Vehicle Class Counts

In order to make the comparison analysis more reliable, this study examined the vehicle counts made by WIM and TIRTL during a duration of 24 hours. Presented in Table 4-3 are the daily vehicle class counts made by WIM and TIRTL on five individual days, including three days in 2008 and two days in 2009. Class 0 represents those vehicles that could not be classified by WIM. For TIRTL, Class 0 represents those vehicles under Class 14 and Class 15. Also presented in Table 4-3 are the percent errors (P.E.) between the WIM and TIRTL daily vehicle counts, and other information such as average speed (V) and weather conditions.

Table 4-3 Comparison of WIM and TIRTL Daily Vehicle Class Counts

Vehicle Class	**8/1/08**		**9/4/09**		**12/23/08**		**1/1/09**		**5/1/09**	
	WIM	TIRTLE	WIM	TIRTLE	WIM	TIRTLE	WIM	TIRTLE	WIM	TIRTLE
0	2282	1	7861	2	2517	3	712	0	680	2
1	502	975	115	782	118	511	98	41	82	245
2	20599	29897	9596	16577	10414	13690	10514	19035	24519	29233
3	16634	8825	10685	6088	11030	4319	9835	3905	12745	7623
4	270	721	215	564	145	440	56	70	215	313
5	4417	1386	3651	1386	2845	1030	2336	141	1474	1058
6	575	576	296	459	226	188	98	95	438	388
7	244	133	11	59	31	19	15	12	39	28
8	555	941	317	1073	283	562	104	112	478	1036
9	10054	9662	8166	10185	6704	4716	3072	3272	10048	7936
10	49	171	48	262	29	117	5	31	49	188
11	781	817	545	627	483	450	46	57	820	624
12	194	208	137	160	126	117	34	41	237	172
13	3	19	2	28	5	14	1	7	5	36
Total	57159	54332	41645	38252	34956	26176	26926	26819	51829	48882
P. E.	4.9%		8.1%		25.1%		0.4%		5.7&	
V, mph	68	65	68	64	56	56	71	71	67	68
Weather	Fog, Clear, haze, Cloudy		Rain, Overcast, Cloudy, haze		Overcast, Snow, Freezing Rain		Clear, Cloudy, Overcast		Rain, Overcast, Cloudy	

The total daily vehicle counts by TIRTL agree well with the total daily vehicle counts by WIM, except December 23, 2008 when the percent error reached 25%. However, the overall average speeds agree very well on December 23, 2008. While overcast, snow, and freezing rain were observed on December 23, 2008, and while the average speeds reduced greatly, it remains unclear, at this time, why the total daily vehicle counts by WIM and TIRTL differed greatly. The unclassified vehicle count might be very large and become an issue associated with WIM vehicle classification. Under Class 2 (passing cars), the vehicle class count by TIRTL is always greater than that by WIM. Under Class 3 (van and pick-up truck), however, the vehicle class count by TIRTL is always less than that by WIM. It was also observed that under Class 5 (single unit truck), the vehicle class count by TIRTL is always much less than that by WIM.

The above observations confirm previous research findings reported elsewhere (28, 29), which indicate that great discrepancies existed between the vehicle counts under Classes 2, 3 and 5 by TIRTL and other vehicle classifiers. To the authors' knowledge, it appears that the vehicle counts of Class 5 by TIRTL are more reasonable. This is because as shown in Tables 4-1 and 4-2, the vehicles under Category 2 approximately account for 4.6% (manual counts) or 4.7% (video counts) of the total vehicle counts. Since Category 2 consists of all vehicles under Classes 4, 5, 6, and 7, the actual vehicle counts under Class 5 should be less than 4.6% or 4.7%. As shown in Table 4-3, Based on the vehicle counts in Table -4-3, the vehicle counts under Class 5 by WIM account for 7.5% of the total vehicle counts by five-day average. However, the vehicle counts under Class 5 by TIRTL constitute 2.6% of the total vehicle counts by average.

Vehicle Class Distributions

In order to avoid possible concerns over the accuracy of WIM vehicle counts, this study further computed the vehicle class distributions from the WIM and TIRTL vehicle class counts. The vehicle class distribution is the variation of the percentages of vehicle class counts and indicates how large one vehicle class count is in relative to the other vehicle class counts. At a specific location on a certain road, the vehicle class distribution represents the relative values and should not exhibit abrupt changes from time to time even though the total vehicle count may change from time to time. In addition, the vehicle class distribution can find many applications in highway project economic analysis, crash analysis, asset management, and pavement design. As presented in Figure 4-4 are the vehicle class distributions computed from WIM and TIRTL vehicle counts, respectively.

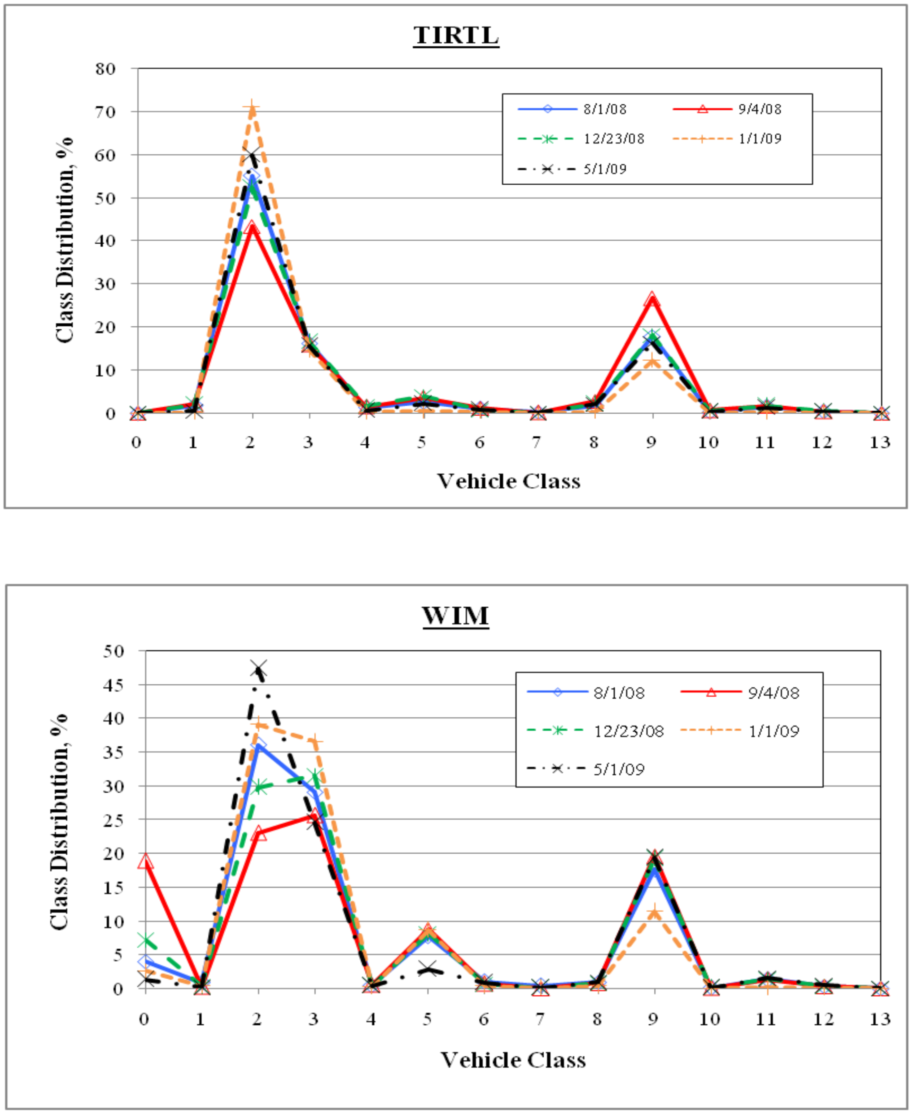

Figure 4-4 Vehicle Class Distributions by WIM and TIRTL

Apparently, discrepancies exist between the WIM and TIRTL vehicle class distributions. First, the vehicle class distributions from TIRTL vehicle counts exhibit two outstanding peaks, one at Class 2, and the other at Class 9. However, the vehicle class distributions from WIM vehicle counts demonstrate more peaks and spread more evenly. Second, in the case of two-axle, four-tire vehicles, i.e., all vehicles under Classes 2 and 3, the passenger cars (Class 2) are the dominant vehicle type for TIRTL. Nevertheless, the other two-axle, four-tire vehicles, including pickups and vane, may be more than the passenger cars for WIM. This implies that TIRTL may work better than WIM to distinguish Class 3 from Class 2. Third, much more vehicles were classified as Class 5 by WIM than by TIRTL.

The default truck class distributions (30) were also utilized to validate the TIRTL and WIM vehicle class distributions. Figure 4-5 shows a comparison of vehicle class distributions among TIRTL, WIM and other sources. TTC-1, TTC-2 and TTC-4 indicate the default truck class distribution for major single-trailer truck routes under Type I, Type II, and Type III, respectively. The truck class distribution for TIRTL or WIM is the average distribution determined from Figure 4-4. Again, the percentage of Class 5 by WIM is greater than those by TIRTL and default values. Overall, the truck class distribution determined by TIRTL agrees with the default distributions better than that by WIM. While it is difficult to confirm whether TIRTL or WIM provides better performance, it appears that TIRTL can provide vehicle classification information with accuracy not worse than WIM.

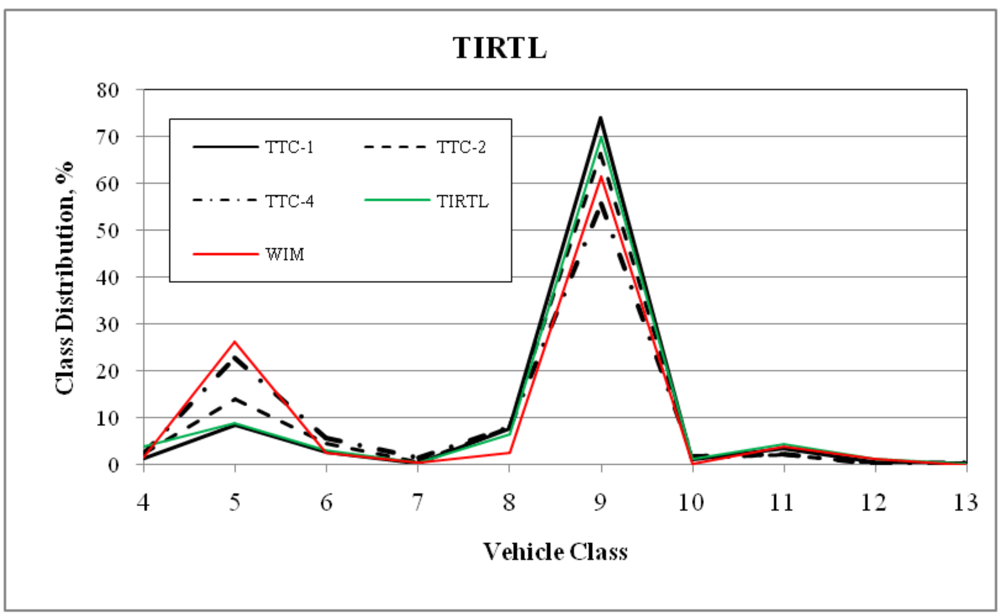

Figure 4-5 Comparison of Truck Class Distributions

Chapter 5

IMPACT OF WEATHER CONDITIONS ON TIRTL'S PERFORMANCE

The TIRTL System Operations

It is well known that the TIRTL system utilizes infra-red light technology to detect vehicle information needed to count and classify passing vehicles. The detection method can be illustrated using Figure 5-1 (31). When a TIRTL system is in operation, the transmitter emits two parallel and two cross infra-red light beams that traverse across the roadway to the receiver on the opposite side of the roadway. While a vehicle passing between the transmitter and receiver, each wheel interrupts and breaks each of the four light beam pathways. Breaking of a light beam is called a Break Beam Event. Re-establishment of the broken light beam's continuity is called a Make Beam Event. The receiver detects the precise time of each Beam Event. The speed is measured according to the parallel beam breaking. The vehicle classification is performed on the basis of axle counts and inter-axle spacings. The lane identification is accomplished on the basis of both parallel and cross beam beaks.

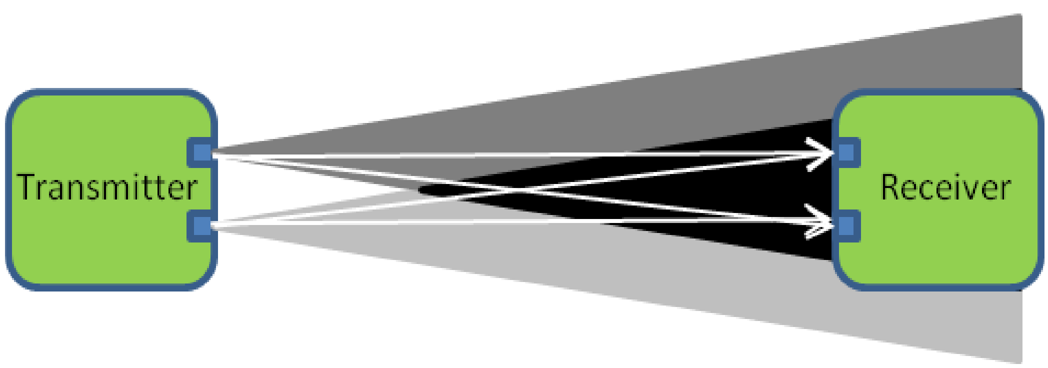

Figure 5-1 Configuration of TIRTL Infra-Red Light Beams

It is highlighted that by the TIRTL vendor, the alignment of the transmitter and receiver units plays a critical role. The beams traversing the roadway should be set at a point as low as possible so as to reduce the interference from mud-flaps and other features hanging from the main body of the vehicles. Since the accuracy of TIRTL system depends largely on the effective detection of the Beam Events between the transmitter and receiver, any disturbance to the light beams by objects other than passing wheels may degrade the system performance. In order to avoid the disturbance to the light beams by vegetation in the median of roadway, the transmitter and receiver can be placed above the pavement at a pre-determined height. However, the possible disturbance to the light beams due to rain and snow remains unknown and needs to be further investigated (28).

Impact of Weather Conditions

<u>Clear Weather</u>

In order to evaluate the potential impacts of adverse weathers on the TIRTL performance, this study examined both TIRTL and WIM data under different weather conditions. Since no manual vehicle counts were available, WIM data was considered as the baseline data. Presented in Table 5-1 are the percent errors between the WIM and TIRTL vehicle counts for Classes 2, 3, 5, and 9 under clear weather conditions. Also presented in Table 5-1 are the percent errors between the total vehicle counts for all 13 classes by WIM and TIRTL. The positive sign, "+", indicates that the TIRTL count is greater than the WIM count, and the negative sign, "-", indicates that TIRTL count is less than the WIM count. As anticipated, the greatest percent error occurred under Class 5, followed by Class 2 and Class 3. Under a given vehicle class except for Class 3, the TIRTL counts may greater or less than the WIM counts. This indicates that the percent errors are random numbers in clear weather. However, the TIRTL counts is always less than WIM counts under Class 3

Table 5-1 Percent Errors in Clear Weather

Class	1/21/09	5/24/09	6/23/09	8/2/08	9/25/08
2	54.5(+)	29.4(+)	51.1(+)	71.7(+)	30.1(-)
3	46.4(-)	38.5(-)	14.7(-)	49.0(-)	69.5(-)
5	33.3(-)	121.7(+)	49.0(+)	81.8(-)	37.2(-)
9	1.2(-)	5.7(-)	39.1(-)	3.6(+)	63.2(-)
All Classes	0.3(-)	14.0(+)	30.7(+)	1.4(+)	45.6(-)

Adverse Weathers

Presented in Table 5-2 are the percent errors between the WIM and TIRTL counts under foggy weather conditions. The greatest percent error arose under Class 2. Under Class 2, the TIRTL counts are greater than the WIM counts. Under Classes 3 and 5, the TIRTL counts are less than the WIM counts. Under Class 9, the TIRTL count is greater than the WIM count on August 6, 2008 and less than the WIM count on January 4, 2009. It looks that the percent errors in foggy weather are greater than those in clear weather. Under All Classes, however, the percent errors in foggy weather are similar to those in clear weather in Table 5. Due to limited data, there is no evidence to indicate the impact of foggy weather.

Table 5-2 Percent Errors in Foggy Weather

Class	8/6/08	1/4/9
2	124.5(+)	58.3(+)
3	4.5(-)	70.5(-)
5	82.8(-)	81.8(-)
9	13.7(+)	60.4(-)
All Classes	11.2(+)	39.1(-)

Table 5-3 shows the percent errors between TIRTL and WIM counts in normal snowy weather. The TIRTL counts are greater the WIM counts under some classes, and less than the WIM counts under other classes. No evidence is available to indicate the impact of snow. Again, the TIRTL counts under Class 3 are less than the WIM counts. Tabulated in Table 5-4 are the percent errors in wet weathers, such as normal rainy and thunderstorm weathers. In normal rainy weather, the TIRTL counts are greater than the WIM counts in some cases, and less than the WIM counts in other cases. As anticipated, the TIRTL counts are less than the WIM counts under Class 3. No specific pattern can be identified in the variations of the percent errors.

In thunderstorm weather, the TIRTL counts are always less than the WIM counts regardless of vehicle class and survey date. Compared to all other weathers, it looks that the percent errors in thunderstorm weather are very large. Class 9 witnessed the greatest percent errors, followed by Class 3. Even the overall percent errors for All Classes are very high and close to 95%. It can be concluded that in thunderstorm weather, the TIRTL system may undercount vehicles. This agrees with a finding by another study (28), which indicated that severe weather affects the TIRTL sensor's performance and causes traffic to be undercounted.

Table 5-3 Percent Errors in Normal Snowy Weather

Class	8/6/08	1/4/09
2	23.8(+)	72.9(+)
3	63.3(-)	45.1(-)
5	62.7(-)	76.6(-)
9	40.3(-)	6.2(+)
All Classes	42.3(-)	0.2(-)

Table 5-4 Percent Errors in Wet Weather

Class	Normal Rainy Weather				Thunderstorm Weather			
	8/23/08	9/4/08	5/1/09	6/18/09	3/13/09	5/15/09	6/1/09	8/5/08
2	57.4(+)	14.9(+)	0.7(-)	16.7(-)	88.9(-)	96.7(-)	27.1(-)	68.1(-)
3	48.7(-)	60.3(-)	47.2(-)	40.4(-)	92.7(-)	98.2(-)	54.3(-)	87.2(-)
5	22.7(-)	25.6(-)	23.7(+)	23.5(+)	81.6(-)	79.3(-)	40.8(-)	91.7(-)
9	12.8(-)	54.5(-)	80.8(-)	82.3(-)	100.0(-)	100.0(-)	61.9(-)	100.0(-)
All Classes	0.7(+)	27.8(+)	22.0(+)	36.1(+)	92.4(-)	94.9(-)	42.3(-)	87.5(-)

Chapter 6

CONCLUSIONS

Video Vehicle Detection and Classification

The digital image based vehicle monitoring and classification system developed by this study is user friendly and can be easily to setup, and perform data acquisition, vehicle monitoring, and length-based vehicle classification. This system can help develop the models for correcting weigh-in-station data, in particular the unclassified vehicle counts. It was shown that the traditional method to treat all unclassified vehicle counts as trucks is too conservative and will largely overestimate the truck traffic volume. Video technologies can provide accurate and effective vehicle detection when vehicles are classified into four categories, including two-axle, four-tire vehicles, single unit trucks, single-trailer trucks, and multi-trailer trucks.

WIM Vehicle Detection and Classification

WIM sensor malfunction can generate serious vehicle classification issues. The percentage of unclassified vehicles increases as vehicle counts increases. As the number of travel lanes increases, the possibility for vehicles to execute lane changing or passing increases. Therefore, more vehicles may occupy two adjacent lanes or change speeds on sensors, leading to greater percentages of unclassified vehicles. It becomes unacceptable when the percentage of unclassified vehicles exceeds 4% for a single lane.

Based on the WIM data statewide, the unclassified vehicles mainly involved single tractor trailers and passenger cars. Single unit trucks were most likely classified by WIM. While traffic volume and lane number are the two main contributing factors, it is unrealistic to predict the unclassified vehicles in terms of traffic volume and lane number at this time. Overall, vehicles under Categories 1, 2, 3, and 4 account respectively for 35%, 5%, 48%, and 12% of the total unclassified vehicles.

TIRTL Vehicle Detection and Classification

Under clear weather conditions, the TIRTL vehicle counts agreed very well with the manual and video vehicle counts, respectively. When vehicles are classified into four categories, such as two-axle, four-tire vehicles, single unit trucks, single-trailer trucks, and multi-trailer trucks, the accuracy of vehicle classification for Category 1, including all two-axle, four-tire vehicles, was better than that for tractor trailers. WIM vehicle counts were utilized to validate the performance of TIRTL system. Unlike WIM system, the number of unclassified vehicles by TIRTL was very small.

For axle-based vehicle classification, i.e., the 13-class FHWA vehicle classification scheme, great discrepancies existed between the WIM and TIRTL vehicle class counts. Both WIM and TIRTL demonstrated difficulties to distinguish Class 3 from Class 2. However, TIRTL demonstrated better performance to identify vehicles under Class 3 than WIM, regardless of weather conditions. Under Class 5, the TIRTL vehicle counts were more reasonable than the WIM vehicle counts. The WIM system might over-count vehicles under Class 5. Based on the default truck class distributions, TIRTL might provide vehicle classification more accurate than WIM. Under normal weathers, fog, snow, and rain did not affect TIRTL's performance. Under thunderstorm weather, however, TIRTL might undercount vehicles regardless of vehicle class.

References

(1) Mechanistic-Empirical Pavement Design Guide, Interim Edition: A Manual of Practice Manual, American Association of State Highway and Transportation Officials, Washington, DC, July, 2008.

(2) Office of Highway Policy Information, *Traffic Monitoring Guide*, Federal Highway Administration, U.S. Department of Transportation, 2001.

(3) Shuo Li, Tommy Nantung, and Yi Jiang (2005). "Assessing issues, technologies, and data needs to meet traffic input requirements by M-E pavement design guides: Implementation Initiatives." Transportation Research Record 1917, Journal of the Transportation Research Board, 141-148.

(4) Andrew P. Nichols and Darcy M. Bullock, Quality Control Procedures for Weigh-in-Motion Data, JTRP Preliminary Draft, Purdue University, 2004.

(5) TIRTL*soft* V1.19 User Manual–Edition1.1.0, Control Specialists Company, Winter Park, FL 32789.

(6) D. Beymer, P. Mclauchlan, B. Coifman, and J. Malik (1997). "A real-time computer vision system for measuring traffic parameters." Proc. of IEEE Conf. Computer Vision and Pattern Recotniion, 496-501.

(7) D. Koller, J. Weber, and J. Malik (1994). "Robust multiple car tracking with occlusion reasoning." Proc. of ECCV, 189-196.

(8) K. P. Karmann, and A. Von Brandt (1990). "Moving object recognition using an adaptive background memory." Proc. of Time-Varying Image Processing and Moving Object Recognition, Vol. 2.

(9) O. Masoud, N.P. Papanikolopoulos, and N. Kwon (1997). "Vision-based monitoring of weaving sections." Proc. of IEEE Conf. Intelligent Transportation Systems, 338-343.

(10) S. Gupte, O. Masoud, R. F. K. Martine, and N. P. Papanikolopoulos (2002). "Detection and Classification of Vehicles." IEEE Transactions on Intelligent Transportation Systems, 3(1), 37-47.

(11) B. Bhanu, S. Lee, and S. Das (1995). "Adaptive image segmentation using genetic and hybrid search methods." IEEE Trans. Aerosp. Electron. Syst., 31(4), 1268-1290.

(12) C.-S. Fuh, S.-W. Cho, and K. Essing (2000). “Hierarchical color image region segmentation for content-based image retrieval system.” IEEE Trans. Image Processing, 9(1), 156-162.

(13) J. Chen, T.N. Pappas, A. Majsilovic, B.E. Rogowitz (2005). “Adaptive perceptual color-texture image segmentation,” IEEE Trans. Image Processing, 14(10), 1524-1536.

(14) T. Gevers, “Image segmentation and similarity of color-texture objects (2002).” IEEE Transactions on Multimedia, 4(4), 509-516.

(15) S. Sun, D. R. Haynor, Y. Kim (2003). “Semiautomatic video object segmentation using vsnakes,” IEEE Trans. Circuits and Systems for Video Technology, 13(1).

(16) M. E. Farmer and A. K. Jain (2005). “A wrapper-based approach to image segmentation and classification,” IEEE Trans. Image Processing, 14(12), 2060-2072, 2005.

(17) Design and Construction Reference Guide. Indiana Department of Transportation, 2007.

(18) Y. Du, C.I Chang, and P.D. Thouin (2003). "Automated system for text detection in individual video Images.” Journal of Electronic Imaging, Vol. 12, No. 3, 410-422.

(19) R.O.Duda, P.E. Hart, and D.G. Stork, Pattern Classification, 2nd Edition, Wiley Interscience: New York, 2000.

(20) http://en.wikipedia.org/wiki/File:Axonometric_projection.svg.

(21) http://www.britannica.com/EBchecked/topic/478486/projective-geometry.

(22) Bill McCall, and W. C. Vodrazka, Jr. (1997). States’ Successful Practices Weigh-In-Motion Handbook, CTRE, Iowa State University.

(23) Manual on Uniform Traffic Control Devices, 2003 Edition, Federal Highway Administration, U.S. Department of Transportation.

(24) Best Practices Guidebook: Collecting Short Duration Manual Vehicle Classifications Counts on Highway Volume Urban Facilities, Carter and Burgess, Inc., Denver, CO 80202, 2005.

(25) Nikiforos Stamatiadis and David L. Allen (1997). “Seasonal factors using vehicle classification data.” Transportation Research Record 1593, Journal of the Transportation Research Board, 23-28.

(26) Battelle Memorial Institute (2004). Traffic Data Quality Measurement, Final Report. Work Order Number BAT 03-007. 505 King Avenue, Columbus, Ohio 43201.

(27) ASTM Designation E 1318-02. Standard Specification for Highway Weigh-In-Motion (WIM) Systems with User Requirements and Test Methods, ASTM 04.03.

(28) Jerry Kotzenmacher, Erik Minge, and Bingwen Hao (2005). Evaluation of Portable Non-Intrusive Traffic Detection System, Final Report, 2005-37, Minnesota Department of Transportation.

(29) Xin Yu (2009). "Evaluation of non-intrusive sensors for vehicle classification on freeways." 2nd International Symposium on Freeway and Tollway Operations, June 21-24, 2009, Honolulu, Hawaii.

(30) Guide for Mechanistic-Empirical Design of New and Rehabilitated Pavement Structures, NCHRP 1-37A, Final Report, ERES Consultants Division, ARA Incorporation, March 2004.

(31) TIRTL*soft* V1.19 for Windows: User Manual, Doc: TSUM 001, Edition: 1.1.0, CEOS Industrial Pty. Ltd., Unit 3, 17 Burgundy Street, Heidelberg, Victoria, 3084, Australia.